

Locational Marginal Network Tariffs for Intermittent Renewable Generation*

Thomas P. Tangerås[†] and Frank A. Wolak[‡]

November 29, 2019

Abstract

The variability of solar and wind generation increases transmission network operating costs associated with maintaining system stability. These ancillary services costs are likely to increase as a share of total energy costs in regions with ambitious renewable energy targets. We examine how efficient deployment of intermittent renewable generation capacity across locations depends on the costs of balancing real-time system demand and supply. We then show how locational marginal network tariffs can be designed to implement the efficient outcome for intermittent renewable generation unit location decisions. We demonstrate the practical applicability of this approach by applying our theory to obtain quantitative results for the California electricity market.

Key words: Ancillary services costs, efficiency, locational marginal network tariffs, renewable electricity generation, system stability

JEL: L94, Q20, Q42

*We would like to thank Ramteen Sioshansi and participants at The Eleventh Conference on The Economics of Energy Markets and Climate Change (2017) in Toulouse for their comments. This research was conducted within the "Economics of Electricity Markets" research program at IFN. Financial support from the Swedish Energy Agency (Tangerås) and the Department of Energy (Wolak) is gratefully acknowledged.

[†]Research Institute of Industrial Economics (IFN) P.O. Box 55665, 10215 Stockholm, Sweden. Affiliate researcher, Energy Policy Research Group, University of Cambridge. Faculty affiliate, Program on Energy and Sustainable Development, Stanford University. E-mail: thomas.tangeras@ifn.se.

[‡]Program on Energy and Sustainable Development and Department of Economics, Stanford University, 579 Serra Mall, Stanford, CA 94305-6072. E-mail: wolak@zia.stanford.edu

1 Introduction

The intermittency of solar and wind generation increases the cost of maintaining system stability and reliability. Examples of such *ancillary services costs* include automatic generation control, spinning reserves, non-spinning reserves, and fast ramping reserves. Historically, the share of intermittent renewable generation capacity in most jurisdictions was small, which meant that allocating ancillary services costs across consumers and/or producers in an arbitrary manner did not result in significant economic efficiency losses. However, in many regions ancillary services costs have become increasingly important with the surge in intermittent renewable energy production brought about by renewable energy mandates.

In California, for example, annual ancillary services costs more than tripled from 2015 to 2018.¹ The primary driver of these changes was the nearly 5,800 MW increase in grid scale solar generation capacity and more than 500 MW increase in wind generation capacity that came on line between 2015 and the end of 2018.² California has a 33 percent renewable portfolio standard (RPS) by 2020 and a 50 percent RPS by 2030, so ancillary services quantities and ancillary services costs are likely to become an even larger share of total wholesale energy costs in the future.

These trends in ancillary services quantities and costs are common to all regions with significant intermittent renewable energy goals. They provide strong evidence that the economic efficiency consequences of continuing to allocate ancillary services costs in an arbitrary manner are increasing. We propose to internalize these ancillary services cost increases through network tariffs that price locational differences in the factors driving these costs. Specifically, different dollar per MW of capacity installed network tariffs would be assessed for intermittent renewable resources interconnecting at different renewable resource locations in the transmission grid. Keeping other factors the same, these *locational marginal network tariffs* should encourage renewable generation unit interconnection at locations that minimize the adverse market efficiency consequences of meeting a region's intermittent renewable energy goals.

This paper develops a theoretical model to characterize the socially efficient expansion of intermittent renewable generation capacity needed to achieve a specified renewable energy target (such as California's 33 percent renewable energy goal) in a manner that accounts for the grid reliability externality associated with the necessary intermittent generation investments.³ By subtracting the first-order condition for a generation unit owner's capacity expansion decision at a location in the grid and the first-order conditions from the socially efficient investment solution at that same lo-

¹California Independent System Operator, 2016 Annual Report on Market Performance and Issues, p. 8, available at <https://caiso.com/Documents/2016AnnualReportonMarketIssuesandPerformance.pdf> and 2018 Annual Report on Market Performance and Issues, p. 2, available at <https://caiso.com/Documents/2018AnnualReportonMarketIssuesandPerformance.pdf>.

²California Independent System Operator, 2018 Annual Report on Market Performance and Issues, p. 53, available at <https://caiso.com/Documents/2018AnnualReportonMarketIssuesandPerformance.pdf>.

³This grid reliability externality exists because renewable generation entrants do not take into account the increased ancillary services costs associated with their locational entry decisions.

cation, we derive an expression for the dollars per MW installed locational marginal network tariff that implements the socially efficient allocation of renewable generation as a decentralized market outcome.

We then use market outcome and hourly generation data from the California ISO control area to estimate features of the joint distribution of hourly capacity factors for all renewable resource areas in California and the other parameters of our model. Based on those estimates, we compute two socially efficient investment solutions (one constraining investment at each location to be at least the current capacity at that location and the other only requiring non-negative capacities at all locations) and the optimal locational marginal network tariffs associated with each solution. Finally, we compute several alternative solutions to achieving California’s renewable energy goals and compare the costs of attaining those goals under these solutions to the costs under our two efficient solutions.

The central planner’s problem is how to distribute incremental or total intermittent capacity across renewable resource locations in a control area so as to minimize the total expected cost of serving demand, subject to achieving an annual expected output target for renewable energy production. This problem is very similar to a portfolio selection problem in which a manager distributes investment dollars across financial assets to minimize the variance of returns, subject to achieving a given expected return. There are two major differences between the renewable generation investment problem and the classical portfolio choice problem. First, short sales are impossible because capacity at each location must be non-negative. In the incremental capacity expansion problem, existing capacity at that location is sunk. Second, the socially efficient renewable generation capacity investment portfolio depends also on factors other than the variance and covariance of asset returns, for instance the covariance with consumption. This second feature is likely to be important in reality because some intermittent generation technologies are better suited to meet peak demand than others. For example, solar generation capacity in California produces the most energy during daylight hours versus wind generation capacity that tends to produce more energy in the early morning and late evening hours.

We show that implementing the efficient allocation of solar and wind power as a decentralized equilibrium, requires a locational marginal network tariff that covers both the marginal cost of connecting the capacity to the grid at that location and the marginal expected ancillary services cost of the capacity. Locational investment decisions by intermittent renewable resources can be distorted for reasons besides a failure to internalize marginal network costs. For instance, the marginal subsidy to a renewable generation investment can differ from the marginal social value of contributing to the renewable target. If so, the locational marginal network tariff can be used as an instrument to correct these distortions as well.

We present a stylized application of our modeling framework to the California electricity market, to demonstrate the feasibility and practicality of implementing locational marginal network tariffs. We focus on the role of system stability in relation to renewable generation investment by estimating

the marginal network tariffs associated with internalizing the marginal expected ancillary services costs at each location. One should be careful about drawing general conclusions from this stylized analysis, but we believe several of our conclusions are likely to hold even with a more realistic model. First, we find significant differences across locations in terms of the efficient marginal network tariffs. They differ by multiples as high as four to one across renewable resource locations, and the marginal tariffs at solar locations are qualitatively different from those at wind locations, with the latter locations displaying much more variability. Because investments at particular locations can contribute to system stability, the efficient marginal network tariffs can be below the marginal costs of connecting capacity to the grid at such locations.

The marginal network tariffs associated with internalizing the marginal expected ancillary services costs are modest in absolute numbers, below \$2,200 per MW installed capacity per year at most locations. This suggests that locational marginal network tariffs can incite renewable owners to make efficient localization decisions without substantially reducing the overall profitability of investments. The differences in tariffs are likely to be amplified and the overall tariffs are likely to somewhat increase when even more renewable generation is brought on line and ancillary services costs increase even further. These results support the view that locational marginal network tariffs can yield a cost-effective approach for regions with ambitious renewable generation capacity expansion goals.

This is the first paper to propose locational marginal network tariffs as an instrument to internalize the increase in system operating costs and correct other distortions in the location decisions of new intermittent renewable generation units, and to characterize the efficient design of such tariffs. We are the first to assess efficient deployment of solar and wind generation capacity based on non-simulated data, and we do this for the California electricity market. We also estimate the locational marginal network tariffs that can sustain the efficient solution. Callaway et al. (2018) and Sexton et al. (2018) examine renewable energy subsidies in the US in relation to greenhouse gas emissions and other pollutants based on simulated production data for wind and solar power. Lamp and Samano (2019) apply our approach to evaluate the efficiency of solar power expansion in Germany, based on non-simulated data.⁴ None of those papers discuss the role of network tariffs for renewable investment.

The remainder of the paper proceeds as follows. Section 2 characterizes the growing renewable generation intermittency challenge facing California. Section 3 presents our theoretical modeling framework and derives the socially efficient renewable energy investment solution for meeting a given renewable energy goal. This section then uses this modeling framework to characterize the efficient locational marginal network tariff for renewable resources. Section 4 contains our application to the California electricity market and derives two socially efficient solutions to meeting California's 33

⁴A number of papers use mean-variance portfolio theory to minimize wind variability in simulated models of wind power location decisions, for instance Novacheck and Johnson (2017) for the US Midwest, Shahriaria and Blumsack (2018) for the Eastern US and Tejada et al. (2018) for Europe.

percent RPS along with the computed locational marginal network tariffs that internalize marginal system costs. Section 5 considers several counterfactuals that illustrate the increased cost of meeting California’s RPS goal using plausible non-optimal policies for intermittent renewable generation capacity expansion. Section 6 concludes the paper with a brief policy discussion. All tables and figures are in the Appendix.

2 California’s Renewable Generation Challenge

California has invested in over 11,000 MW of grid-scale solar generation capacity and over 4,400 MW of grid-scale wind generation capacity between 2002, when the state’s RPS was first implemented, and the end of 2018.⁵ For solar capacity, virtually all of this investment has taken place since 2011, whereas for wind this investment has occurred at a steady annual rate since 2002. As of the beginning of 2019, there was more than 14,000 MW of grid-scale solar generation capacity and more than 6,000 MW of wind capacity in California. Figure 1 shows the cumulative installed capacity of solar and wind generation in the California ISO control area from 2010 through 2018.

Figure 2 plots the histogram of hourly wind output in the California ISO control area for 2018 conditional on a positive value of hourly wind output. This histogram is extremely skewed to the right and has a substantial amount of frequency mass close to zero hourly output. The histogram rapidly decreases to zero frequency more than 2,000 MWh below the installed capacity of wind units in the state.

Hourly solar output was equal to zero in more than 42 percent of the hours in 2018. Figure 3 plots the histogram of hourly solar output conditional on a positive value of hourly solar output. This histogram is bimodal, with one peak very close to zero and another smaller peak close to 9,000 MWh. With the exception of very low hourly output levels, the distribution of hourly solar output levels is relatively flat across all output levels. Different from the case of wind capacity, there are a number of hours in 2018 when the hourly solar output was closer to the amount of installed solar generation capacity in the California.

Figure 4 plots the histogram of the sum of hourly wind and solar output for 2018 conditional on this sum being positive. Less than one-tenth of one percent of the hours in 2018 no wind nor solar energy was produced. This histogram is tri-modal, with the largest frequency at very low levels of hourly output. There is second spike at 3,000 MWh and another smaller one at 9,000 MWh. This histogram also has a very significant right skew.

How has this distribution changed over time as California has expanded the amount of solar and wind generation capacity? One might expect that as more renewable resource locations are developed, the uncertainty in aggregate hourly wind, solar, and wind and solar output should decline. This intuition is based on the logic that there is little contemporaneous correlation between

⁵California Energy Commission–Tracking Progress available at https://ww2.energy.ca.gov/renewables/tracking_progress/documents/renewable.pdf.

hourly renewable energy output at different resource locations in California. However, as shown in Wolak (2016), there is a substantial amount of contemporaneous correlation between the hourly output of solar locations in California and between the hourly output of wind locations in California.

Wolak (2016) uses one year of hourly output data from all wind and solar units in California between April 1, 2011 and March 31, 2012 and computes the capacity factor f_{jh} at location j during hour h for all hours of the year as $f_{jh} = \frac{Q_{jh}}{K_j}$, where Q_{jh} is the hourly output in MWh at renewable energy location j during hour h and K_j is the amount of renewable generation capacity in MW at location j . Wolak (2016) then computes the contemporaneous covariance matrices of the hourly capacity factors of all 13 solar locations, all 40 wind location and all 53 wind and solar locations that existed during his same period. An eigenvalue decomposition of these covariance matrices reveals that more than 80 percent of the sum of variances in hourly capacity factors across the 13 solar locations can be explained by a single factor. For the 40 wind locations, more than 80 percent of the sum of the variances in the hourly capacity factors across these locations can be explained by three orthogonal factors. For the 53 wind and solar locations, more than 80 percent of the sum of the variances in the hourly capacity factors across these locations can be explained by 5 orthogonal factors.

Wolak (2016) argues that these results demonstrate that adding more renewable generation capacity in California is likely to increase significantly the aggregate uncertainty in renewable energy output. To demonstrate this point, Wolak (2016) computes the annual sample mean and covariance of the vector of hourly capacity factors across all renewable energy locations in California to derive the efficient frontier of portfolios of renewable generation capacity investments with the same total installed capacity of wind and solar generation units in California, but with every portfolio on this efficient frontier having the largest mean hourly capacity factor for the given portfolio standard deviation of the hourly capacity factor. The actual portfolio of wind and solar generation units in California is shown to lie significantly inside this efficient frontier, which indicates the significant potential reliability and economic benefits of locational network tariffs as a mechanism for reducing the variability in aggregate hourly renewable output and the costs of managing system reliability.

Table 1 reports the annual mean, standard deviation, Coefficient of Variation (CV), standardized skewness, and standardized kurtosis of the hourly wind, solar and combined wind and solar output for 2013 to 2018.⁶ Standard deviations increase across all years and all three types of hourly output. This is consistent with the amount of installed renewable generation capacity increasing across the years. The sample CV provides a normalized measure of the variability in the three hourly output measures that accounts for the growth in the annual mean hourly output across the years. Consistent with the results reported in Wolak (2016), the general trend for the combined solar and wind output is that CV has increased every year between 2013 and 2018. The standardized

⁶If Q_h is the output in hour h , \bar{Q} is the annual mean of hourly output and s is the annual standard deviation of hourly output, then the Coefficient of Variation is equal to s/\bar{Q} , the standardized skewness is equal to $1/H \sum_{h=1}^H (Q_h - \bar{Q})^3 / s^3$, and the standardized kurtosis equals $1/H \sum_{h=1}^H (Q_h - \bar{Q})^4 / s^4$, where H is the number of hours in a year.

skewness of the annual distribution of hourly output of wind and solar resources has also increased across the years.

The duration of low hourly renewable output levels is an important measure of intermittency that signals the need for system operators to purchase more ancillary services as the share of intermittent renewable resources increases. For each year from 2013 to 2018, we choose an hourly output level, say 500 MWh. Starting with hour one of January 1 of the year, we look for the first hour with an output of wind, solar, or wind and solar energy production below this level. We count how many consecutive hours the hourly output remains below this level. This counts as one duration of output levels below the 500 MWh threshold. We then record the length of this duration in hours. We repeat this same process of finding spells of hourly output less than 500 MWh for all hours of the year. Table 2 reports the number of durations of low hourly output of wind for 500, 1,000, 1,500 and 2,000 MWh threshold values. The length of these durations in hours and the standard deviation of these durations, as well as the maximum length duration is reported. Particularly, for the earlier years in the sample, there are extremely long maximum periods of low renewable output. Even by 2018, when there is more than 6,000 MW of wind capacity in California, the maximum duration of less than 2,000 MWh of wind output was 377 hours, which is almost 16 days. Table 3 reports Table 2 for solar output. The maximum duration of low levels of solar output are significantly smaller than those for wind output, consistent with the fact that there is fixed number of daylight hours each day of the year and even during cloudy days, some solar energy is produced.

Table 4 reports Table 2 for the combined hourly wind and solar output for 1,000, 2,000, 3,000, and 4,000 MWh hourly output thresholds. Comparing the 1,000 and 2,000 MWh threshold mean duration, standard deviation, and maximum value in Table 4 to those in Tables 2 and 3 demonstrates that combining these two sources of renewable energy reduces the mean duration of low output levels and maximum duration of low output levels relative to the solar or wind alone. However, there are still substantial durations of low output levels that battery storage technologies would have a difficult time dealing with. For example, in 2018, and although there is more than 18,000 MW of wind and solar capacity in California, the maximum duration of less than 4,000 MWh of output from these units was 65 hours, which is almost three days.

These results provide empirical support for the California ISO's increasing demand for ancillary services as the state has scaled up its wind and solar generation capacity. Further evidence for the increased demand for ancillary services and dispatchable generation capacity is the fact that between 2001 and the end of 2013, California added more than 16,000 MW of natural gas-fired capacity. Figure 5 plots the installed capacity in California by technology as of the end of the years from 2001 to 2018. Although wind and solar investments have made up virtually all of the capacity additions since 2011 and there have been some recent natural gas-fired generation retirements, there is still more than 40,000 MW of natural gas-fired generation capacity in California.

The above analysis of the distribution of the hourly output of wind and solar generation units in California argues that a significant fraction of existing thermal capacity will continue to be needed

to provide ancillary services and energy as California brings on line more renewable generation units to meet its RPS goals. These thermal units must be fully compensated for the services they provide or their owners are likely to mothball or retire them. This compensation will ultimately be paid for by electricity consumers. Our analysis of efficient network tariffs for renewable generation is aimed at minimizing these thermal energy and ancillary services costs associated with meeting California's RPS goals.

3 Optimal Renewable Generation Investment and Tariffs

This section presents our theoretical model of decentralized renewable generation investment. We also characterize the socially efficient renewable generation investment solution, and derive an expression for the locational marginal network tariff that implements the efficient solution under decentralized investment choice.

3.1 Modeling Renewable Generation Investment

Consider a control area with J possible locations of intermittent electricity generation. This energy typically comes from wind and solar generation capacity. Denote by K_j the installed intermittent generation capacity at location j , measured in megawatts (MW), with $\mathbf{K} = (K_1, \dots, K_J)^T$ being the $J \times 1$ vector of intermittent generation capacity at all possible locations, and where T denotes "transpose". Let Q_{jh} be the amount of electricity actually produced at location j during hour $h = 1, 2, \dots, H$, where H is the total number of hours in the year.

Define $f_{jh} = Q_{jh}/K_j$ as the hourly capacity factor at location j during hour h , which is equal to the actual production at location j during hour h divided by the amount that could be produced by full utilization of the K_j MWs of capacity at that location. Let μ_j be the expected value of f_{jh} . The corresponding vector of realized capacity factors during hour h is equal to $\mathbf{f}_h = (f_{1h}, \dots, f_{Jh})^T$, and the expected value of \mathbf{f}_h is equal to $\boldsymbol{\mu} = (\mu_1, \dots, \mu_J)^T$.

In terms of this notation, the actual output Q_{jh} at location j during hour h is equal to $f_{jh}K_j$, and the expected output, $E[Q_{jh}]$, is equal to $\mu_j K_j$. Total renewable energy output during hour h therefore equals $R_h = \sum_{j=1}^J Q_{jh} = \mathbf{f}_h^T \mathbf{K}$, and the expected renewable energy output is $E[R_h] = \boldsymbol{\mu}^T \mathbf{K}$. Let D_h be the realized value of system demand during hour h and $E[D_h]$ its expected value.

The difference between system demand D_h and the intermittent renewable electricity production R_h during hour h yields a residual demand that must be covered by dispatchable generation capacity, primarily thermal generation units. We assume that the total amount of thermal generation capacity at every location is sufficiently large that consumers never have to be curtailed.

Let $C^h(D_h - R_h)$ be the total variable cost of serving the residual demand $D_h - R_h$ for non-renewable resources during hour h . In addition, there is an ancillary services cost $A^h(R_h^w, R_h^s, D_h)$ associated with maintaining system stability, where R_h^w is the output of all wind units during hour

h , R_h^s is the output of all solar units during hour h , and $R_h = R_h^w + R_h^s$.

Assuming that all of the random variables—the elements of the vector \mathbf{f}_h and D_h —have the same stochastic properties across years, the expected net present value (ENPV) of investing one MW of capacity at location j equals:

$$\sum_{\tau=1}^{\bar{\tau}} \sum_{h=1}^H \delta^\tau [z_{jh} f_{jh} - \frac{S^j(\mathbf{K})}{K_j}] - \frac{\bar{F}^j(K_j)}{K_j}, \quad (1)$$

where $\bar{\tau}$ is the life-span in years of the investment, and δ is the annual discount rate. The price z_{jh} paid per unit of renewable output at location j during hour h typically contains a subsidy to the renewable resource owners and therefore can differ substantially from the wholesale price $p_{jh} = P^{jh}(Q_{jh})$. The subsidy often takes the form of a payment per MWh produced that renders the total price of renewable production fixed for the entire term of the power purchase agreement used to finance the construction of the facility: $z_{jh} = z_j$ for all h . We allow the price to depend on the amount of renewable capacity at location j : $z_{jh} = Z^{jh}(K_j)$, with $Z^{jh}(K_j) \leq 0$.

We introduce the term $\frac{S^j(\mathbf{K})}{K_j}$ into (1) to account for our proposed hourly network tariff paid by the investor to the network owner per unit of capacity installed at location j . The tariff should cover the total cost $\bar{N}^j(K_j)$ to the network owner of connecting the K_j MW to the grid as well as the contribution of the facility to total system cost. Hence, we allow the tariff to depend on the installed capacity \mathbf{K} at all locations in the grid.

Finally, $\frac{\bar{F}^j(K_j)}{K_j}$ represents the average capital cost of installing K_j MW of capacity at location j . It encompasses the construction cost plus the discounted expected overhead and maintenance costs over the life-span of the plant. We allow both the network cost $\bar{N}^j(K_j)$ and the capital cost $\bar{F}^j(K_j)$ to be non-linear in K_j to account for scale effects.

The investment is undertaken if and only if it has a non-negative ENPV. Let all payments during the H hours of year τ be made at the end of the year. Normalize the capital cost and the network cost at location j to

$$F^j(K_j) = \frac{\bar{F}^j(K_j)}{H} \frac{1 - \delta}{\delta(1 - \delta^{\bar{\tau}})} \quad \& \quad N^j(K_j) = \frac{\bar{N}^j(K_j)}{H} \frac{1 - \delta}{\delta(1 - \delta^{\bar{\tau}})}.$$

By this normalization, the average hourly ENPV of investing K_j MW of renewable capacity at location j equals

$$\frac{1}{H} \sum_{h=1}^H E[z_{jh} f_{jh} K_j] - F^j(K_j) - S^j(\mathbf{K}). \quad (2)$$

3.2 The Efficient Portfolio of Renewable Generation Capacity

To determine the form of the per MW installed hourly locational network tariff $S^j(\mathbf{K})$, we first solve the central planner's problem and then compare it to the one facing the private investor. The

central planner minimizes the sum of expected thermal energy costs, ancillary services costs and renewable generation investment costs,

$$\frac{1}{H} \sum_{h=1}^H E[C^h(D_h - R_h) + A^h(R_h^w, R_h^s, D_h)] + \sum_{j=1}^J [F^j(K_j) + N^j(K_j)], \quad (3)$$

subject to achieving the renewable portfolio standard (RPS),

$$\frac{1}{H} \sum_{h=1}^H \sum_{j=1}^J E[f_{jh} K_j] = \boldsymbol{\mu}^T \mathbf{K} \geq \alpha \frac{1}{H} \sum_{h=1}^H E[D_h], \quad (4)$$

which requires expected annual hourly renewable energy production to be greater than or equal to 100α ($0 < \alpha < 1$) percent of expected annual hourly electricity demand.

Depending on the problem, we impose the constraint that the installed capacity at location j must be greater than or equal to zero, $K_j \geq 0$, or the installed capacity at location j be greater than or equal to some previously installed capacity K_j^e at location j , $K_j \geq K_j^e$. Let $\mathbf{K}^e = (K_1^e, \dots, K_J^e)^T$ be the vector of existing capacity at all renewable locations. There is also an upper bound $K_j^{up} \geq K_j$ on the amount of capacity that each renewable location can handle because of the configuration of the transmission network. Denote the vector of upper bounds by $\mathbf{K}^{up} = (K_1^{up}, \dots, K_J^{up})^T$.

The Lagrangian for the central planner's problem where investment at all locations must be greater than or equal to the existing capacity at that location and less than or equal to K_j^{up} at each location j , is:

$$\begin{aligned} L(\mathbf{K}, \lambda, \boldsymbol{\xi}, \boldsymbol{\eta}) = & -\frac{1}{H} \sum_{h=1}^H E[C^h(D_h - R_h) + A^h(R_h^w, R_h^s, D_h)] - \sum_{j=1}^J (F^j(K_j) + N^j(K_j)) \\ & - \lambda \left(\alpha \frac{1}{H} \sum_{h=1}^H E[D_h] - \boldsymbol{\mu}^T \mathbf{K} \right) + \boldsymbol{\xi}^T (\mathbf{K} - \mathbf{K}^e) + \boldsymbol{\eta}^T (\mathbf{K}^{up} - \mathbf{K}), \end{aligned} \quad (5)$$

where $\lambda \geq 0$ is the Kuhn-Tucker (KT) multiplier associated with the RPS constraint, $\xi_j \geq 0$ is the KT multiplier associated with $K_j \geq K_j^e$, ($\boldsymbol{\xi} = (\xi_1, \dots, \xi_J)^T$ is the vector of KT multipliers associated with lower capacity investment constraints at the J renewable resource locations), and $\eta_j \geq 0$ is the KT multiplier associated with $K_j \leq K_j^{up}$, ($\boldsymbol{\eta} = (\eta_1, \dots, \eta_J)^T$ is the vector of KT multipliers associated with these J upper bound constraints).

The efficient portfolio \mathbf{K}^* of renewable generation capacity, the shadow price λ^* on the renewable target, and the shadow prices $\boldsymbol{\xi}^*$ and $\boldsymbol{\eta}^*$ at the J locations are jointly characterized by J first-order conditions and $2J + 1$ complementary slackness conditions. The first-order equation for the efficient

investment K_j^* at location j equals

$$\begin{aligned} & \frac{1}{H} \sum_{h=1}^H E[C^{hj}(D_h - R_h^*)f_{jh}] + \lambda^* \mu_j + \xi_j^* \\ & = F^{j'}(K_j^*) + N^{j'}(K_j^*) + \frac{1}{H} \sum_{h=1}^H E\left[\frac{\partial A^h(R_h^{w*}, R_h^{s*}, D_h)}{\partial R_h^w} f_{jh}\right] + \eta_j^* \end{aligned} \quad (6)$$

if j is a wind location, where R_h^{w*} (R_h^{s*}) is total wind (solar) output during hour h given the optimal investment portfolio \mathbf{K}^* , and $R_h^* = R_h^{w*} + R_h^{s*}$ is the corresponding total renewable output. A similar first-order condition applies if j is instead a solar location and we replace $\frac{\partial A^h(R_h^{w*}, R_h^{s*}, D_h)}{\partial R_h^w}$ in (6) by $\frac{\partial A^h(R_h^{w*}, R_h^{s*}, D_h)}{\partial R_h^s}$. The complementary slackness condition of the renewable target is

$$\boldsymbol{\mu}^T \mathbf{K}^* - \alpha \frac{1}{H} \sum_{h=1}^H E[D_h] \geq 0, \quad \lambda^* \geq 0, \quad \lambda^* (\boldsymbol{\mu}^T \mathbf{K}^* - \alpha \frac{1}{H} \sum_{h=1}^H E[D_h]) = 0, \quad (7)$$

and the $2J$ complementary slackness conditions of the lower and upper bounds to capacity are:

$$K_j^* \geq K_j^e, \quad \xi_j^* \geq 0, \quad \xi_j^* (K_j^* - K_j^e) = 0 \quad \forall j \quad \& \quad K_j^* \leq K_j^{up}, \quad \eta_j^* \geq 0, \quad \eta_j^* (K_j^{up} - K_j^*) = 0 \quad \forall j. \quad (8)$$

A marginal increase in the renewable capacity at location j leads to an expected reduction in the use of costly thermal production to cover residual demand. This marginal benefit is the first term on the left-hand side of (6). The second term is the marginal expected contribution to satisfying the renewable target. In an interior optimum, $\xi_j^* = \eta_j^* = 0$, these two marginal benefits are equated with the sum of the marginal capital cost, the marginal grid connection cost and the marginal expected ancillary services cost for the renewable technology installed at location j (wind in this case).

Computing the optimal portfolio of renewable capacity investments assuming that all locations have zero existing capacity simply sets $K_j^e = 0$ for all j . For this case, ξ_j^* is the shadow cost of installing capacity at location j when there is no capacity at location j , and it will be equal to zero if the optimal solution installs any capacity at that location.

Different from the case of the thermal cost of meeting the difference between the hourly demand, D_h , and hourly renewable output, R_h , where one can simply integrate under the aggregate thermal cost curve up to the residual demand for thermal energy, there is no straightforward way to compute the ancillary services costs associated with any possible combination of hourly renewable output and system demand. Consequently, we propose to estimate the expected ancillary services cost in hour h given wind and solar output and system demand, $E[A^h(R_h^w, R_h^s, D_h)]$, using a nonparametric kernel regression using hourly values of total ancillary services costs, TAS_h , wind production, R_h^w ,

solar production, R_h^s , and system demand, D_h . The kernel regression estimate takes the form:

$$E[A(R^w, R^s, D)] = \frac{\sum_{h=1}^{\hat{H}} T A S_h k\left(\frac{R^w - R_h^w}{\sigma_w}\right) k\left(\frac{R^s - R_h^s}{\sigma_s}\right) k\left(\frac{D - D_h}{\sigma_D}\right)}{\sum_{h=1}^{\hat{H}} k\left(\frac{R^w - R_h^w}{\sigma_w}\right) k\left(\frac{R^s - R_h^s}{\sigma_s}\right) k\left(\frac{D - D_h}{\sigma_D}\right)}, \quad (9)$$

where \hat{H} is total sample hours, R^w , R^s and D is point of evaluation of this conditional expectation, $k(t)$ is a univariate kernel, and σ_w , σ_s , and σ_D are smoothing parameters computed using cross-validation. We use the Gaussian kernel, so that $k(t) = \frac{1}{\sqrt{2\pi}} e^{-\frac{1}{2}t^2}$. This functional form flexibly estimates the conditional expectation of total hourly ancillary services costs given the realized values of hourly wind and solar production and total system demand.

With this functional form for $E[A^h(R_h^w, R_h^s, D_h)]$, an expression can be derived for the marginal increase in the expected hourly total ancillary services costs with respect to an increase in wind or solar production at renewable location j that enters into the first-order condition for optimal investment at location j . If location j is a wind location, this expression is $\frac{\partial E[A^h(R_h^w, R_h^s, D_h) f_{jh}]}{\partial R_h^w}$ and if location j is a solar location it is $\frac{\partial E[A^h(R_h^w, R_h^s, D_h) f_{jh}]}{\partial R_h^s}$. We now have all of the ingredients necessary to derive the efficient network tariff for each renewable energy location.

3.3 The Efficient Locational Marginal Network Tariff

To derive an efficient locational marginal network tariff, consider the marginal profitability

$$\frac{1}{H} \sum_{h=1}^H E[(z_{jh}^* + Z^{jh'}(K_j^*) K_j^*) f_{jh}] - F^{j'}(K_j^*) - \frac{\partial S^j(\mathbf{K}^*)}{\partial K_j} \quad (10)$$

of investing an additional MW at renewable resource location j , evaluated at the efficient portfolio \mathbf{K}^* , so that $z_{jh}^* = Z^{jh}(K_j^*)$. The first term is the expected marginal revenue at location j , the second term is the capital cost of the marginal increase in capacity at location j . The third term is the marginal network tariff at location j . Subtracting the marginal profitability condition (10) from (6) for each location yields:

Proposition 1 *We can align the marginal private and social incentives at wind location j (under appropriate concavity assumptions) if and only if the marginal network tariff $\frac{\partial S^j(\mathbf{K}^*)}{\partial K_j}$ at location j is characterized as follows:*

$$\begin{aligned} \frac{\partial S^j(\mathbf{K}^*)}{\partial K_j} &= N^{j'}(K_j^*) + \frac{1}{H} \sum_{h=1}^H E\left[\frac{\partial A^h(R_h^{w*}, R_h^{s*}, D_h)}{\partial R_h^w} f_{jh}\right] \\ &+ \frac{1}{H} \sum_{h=1}^H E[(z_{jh}^* + Z^{jh'}(K_j^*) K_j^* - C^{h'}(D_h - R_h^*) - \lambda^*) f_{jh}] - \xi_j^* + \eta_j^*. \end{aligned} \quad (11)$$

We can align the marginal private and social incentives at solar location j by replacing $\frac{\partial A^h(R_h^{w*}, R_h^{s*}, D_h)}{\partial R_h^w}$ in (11) with $\frac{\partial A^h(R_h^{w*}, R_h^{s*}, D_h)}{\partial R_h^s}$.

Implementing the efficient allocation of wind and solar power as a decentralized equilibrium requires a marginal network tariff $\frac{\partial S^j(\mathbf{K}^*)}{\partial K_j}$ at location j that covers both the marginal cost of connecting the facilities at j to the grid and causes investors to internalize the marginal externality associated with the cost of maintaining system stability. These marginal network and system costs are the two terms on the first row of (11) if j is a wind power location (expressions are qualitatively similar if j is a solar location). The marginal payment to renewable electricity production may differ from the marginal social benefit of that output for a number of reasons. First of all, the wholesale price need not reflect the marginal cost of serving residual demand, for instance because of imperfect competition in the wholesale market. Second, the actual subsidy to renewable investment could be inefficient and differ from the marginal social value λ^* , for instance because the amount of capacity installed at j affects the subsidy. If so, the network tariff must also correct these other distortions, as reflected in the second row of (11).

Assume that z_{jh} paid to renewable output at location j is constant over the life time of the plant and equal to $z_j^* = \frac{1}{H} \sum_{h=1}^H Z^{jh}(K_j^*)$ per MWh produced. Let the wholesale price equal the marginal thermal production cost at every location, so that $p_{jh}^* = C^{hj}(D_h - R_h^*)$. Assume that both the lower bound and upper bound on investment at location j are non-binding, so that both ξ_j^* and η_j^* are equal to zero. In this case, the role of the efficient locational marginal network tariff is to capture the marginal grid connection cost and the expected marginal ancillary services cost, and to correct any distortions associated with the support system for renewable electricity:

$$\frac{\partial S^j(\mathbf{K}^*)}{\partial K_j} = N^{j'}(K_j^*) + \beta_j,$$

where

$$\begin{aligned} \beta_j &= \frac{1}{H} \sum_{h=1}^H E\left[\frac{\partial A^h(R_h^{w*}, R_h^{s*}, D_h)}{\partial R_h^w} f_{jh}\right] + (z_j^* - \lambda^*)\mu_j \\ &+ \frac{1}{H} \sum_{h=1}^H E[Z^{jh'}(K_j^*) f_{jh}] K_j^* - \frac{1}{H} \sum_{h=1}^H E[p_{jh}^* f_{jh}] \end{aligned} \quad (12)$$

if j is a wind location, and we replace $\frac{\partial A^h(R_h^{w*}, R_h^{s*}, D_h)}{\partial R_h^w}$ in (12) with $\frac{\partial A^h(R_h^{w*}, R_h^{s*}, D_h)}{\partial R_h^s}$ if j is a solar location. We can then implement the socially optimal portfolio of renewable capacities \mathbf{K}^* by a locational network tariff

$$S^j(K_j) = N^j(K_j) + \beta_j K_j, \quad (13)$$

for each renewable resource location. The novelty of this network tariff compared to ones that are currently applied, is the β_j term associated with marginal ancillary services costs and price

distortions in renewable subsidies.

4 Application to the California Electricity Market

This section presents a stylized application of our modeling framework to the California electricity market. Before proceeding with this analysis, we would like to emphasize that there are many ways to enhance our model to better reflect actual system conditions in California, but these extensions would either significantly complicate the process of solving our model or require additional data we are currently unable to access. We therefore view the application in this section as a demonstration of the feasibility and practicality of implementing a locational marginal network tariff rather than as finding the correct value for all renewable resource locations in California.

4.1 Data and Estimation of the California Electricity Market

We require three sets of inputs. First, we need estimates of the first two moments of the hourly joint distribution of (\mathbf{f}_h^T, D_h) to compute elements of $E[C^h(D_h - R_h)]$, the expected thermal cost function. Second, we need the information necessary to compute $C^h(D_h - R_h)$, the realized total variable cost of meeting the residual demand with thermal units, for each hour of the year. Third, we need information on the realized value of $A^h(R_h^w, R_h^s, D_h)$ and R_h^w, R_h^s and D_h for a large sample of hours to compute (9). Plugging this information into our model allows us to compute the optimal portfolio of renewable generation investments at all locations in California to achieve the 33 percent RPS goal.

To obtain data on the hourly joint distribution of (\mathbf{f}_h^T, D_h) , we rely on the data used in Wolak (2016), which contains the hourly capacity factor, f_{jh} , for all 13 solar locations and 40 wind locations producing energy and hourly system demand, D_h , during the period April 1, 2011 to March 31, 2012. In terms of the notation of the model, the dimension of the vector, \mathbf{f}_h equals $J = 53$. Section 4 in Wolak (2016) presents a comprehensive analysis of the high degree of contemporaneous correlation between the hourly renewable energy output at all locations in California. This analysis also demonstrates that the hourly outputs of all solar locations are positively correlated with hourly system demand, whereas the outputs at some wind locations are slightly positively correlated with hourly system demand and others are slightly negatively correlated.

For the second set of data, we have compiled the technical characteristics of all thermal generation units operating in California between April 1, 2011 and March 31, 2012. This information includes the heat rate in millions of BTU (MMBTU) per MWh, the nameplate capacity in MW, and variable operating maintenance costs in dollars per MWh. As shown in Figure 5, all thermal capacity in California is natural gas-fired during this time period.

The heat rate HR_g of natural gas-fired generation unit g gives the MMBTUs of natural gas required to produce one MWh of electricity from that unit. We combine this information with the

delivered price of natural gas to generation unit g during day d , $PNATGAS_{gd}$, for each generation unit during our sample period to compute the variable cost of producing a MWh at thermal generation unit g during day d as:

$$VC_{gd} = VOM_g + HR_g \times PNATGAS_{gd},$$

where VOM_g is the variable operating and maintenance cost of unit g . We then compute the hourly system-wide marginal cost curve for the time period April 1, 2011 to March 31, 2012, using the value of VC_{gd} as the height of the step and CAP_g , the capacity in MW of generation unit g as the length of the step, for all generation units that are available to produce electricity during the hour. Stacking these variable cost and capacity steps from the lowest to highest variable cost yields the system-wide marginal cost curve for hour h of day d . Integrating this curve from zero to the value of the residual demand to be served by thermal units, yields the total variable cost of meeting this residual demand.

Although California is currently a significant net importer of electricity, meeting approximately 25 percent of its annual demand from imports, it is likely that it will increasingly export renewable energy during low demand periods with significant in-state renewable energy production. To account for this outcome in our modeling, we allow any excess renewable production in an hour to be sold at the lowest variable cost of any thermal generation unit in California operating during that hour. Because California relies on incremental imports to meet unexpectedly high demand conditions, we also allow California to meet any shortfall between the production of in-state thermal units and system demand by importing electricity at an offer price equal to the highest variable cost unit in California operating during that hour.

The third dataset is a sample of hourly total ancillary services costs, hourly wind energy production, hourly solar energy production, and hourly system demand that can be used to estimate the conditional mean of hourly total ancillary services costs given hourly wind and solar output and hourly system demand. To estimate this model for the highest currently existing renewable penetration in California, we use data from April 1, 2015 to March 31, 2017, to match the same calendar time period as our other data. During this period there are six ancillary services: Regulation Up, Regulation Down, Spinning Reserve, Non-Spinning Reserve, Regulation Mileage Up, and Regulation Mileage Down. For all of these ancillary services, market participants have the option to self-provide from a generation unit they own or have a contract with. For this reason, we follow the convention used by the California ISO Department of Market Monitoring in reporting ancillary services costs, and take the market price, multiply by the total amount of each ancillary service in that hour (the sum of self-procured capacity and capacity purchased from the market) and multiply that sum by the price. Then we sum these amounts over all the ancillary services to obtain total hourly ancillary services costs.

Annual ancillary services costs were \$62 million in 2015, \$119 million in 2016, and \$172 million

in 2017. As percentage of total wholesale energy purchase costs in the California ISO control area, they increased from 0.7 percent to 1.9 percent across the three years. Figures 14 and 15 graph the value of $E[A^h(R_h^w, R_h^s, D_h)]$ as a function of R_h^w and R_h^s for the sample mean of Q_h for different bandwidths. This function is generally increasing in both hourly wind and solar output.

To compute the residual demand faced by thermal resources in California each hour, we must account for the fact that there are other generation technologies in use besides wind, solar and natural gas-fired generation. As shown in Figure 5, there are also small and large hydroelectric units, biomass, geothermal and nuclear power. Small hydro, biomass, and geothermal production count towards the state’s RPS goals. Let the hourly output of these units equal RE_h . Consequently, include RE_h in the computation of the RPS constraint. In terms of this notation, the RPS constraint (4) becomes:

$$\boldsymbol{\mu}^T \mathbf{K} \geq \alpha \frac{1}{H} \sum_{h=1}^H E[D_h] - \frac{1}{H} \sum_{h=1}^H E[RE_h]. \quad (14)$$

We also subtract the hourly production of the sum of nuclear units, large hydroelectric units, and net imports, which we denote QO_h , from hourly system demand D_h . The residual demand for thermal resources then is equal to:

$$QD_h = D_h - QO_h - RE_h - \mathbf{f}_h^T \mathbf{K} \quad (15)$$

The constraint (14) is representative of how the actual RPS mandate applies, and (15) reflects the fact that hydroelectric and nuclear units contribute to meeting demand in California.

The final parameters necessary to solve our model are the \$ per KW of installed capacity cost of building a wind or solar generation unit and the network connection costs. There is considerable debate over the precise value of these costs. We use estimates of these figures of \$2,000 per KW for wind from Anderson et al. (2017) and \$4,000 per KW for solar for all locations from recent data compiled from the California Solar Initiative for systems larger than 1 MW.⁷ We also assume $\delta = 1/(1+r)$ for $r = 0.10$ and a life-span of twenty years, $\bar{\tau} = 20$. The qualitative features of our empirical results are not significantly different for reasonable changes in these parameters. Only the value of λ^* , the shadow price on the RPS constraint at the solution, changed with changes in magnitudes. Higher values of the capacity costs increase λ^* , as do lower values of the discount rate.

4.2 Computed Solutions for the California Electricity Market

We now turn to computing two solutions to the efficient expansion of California’s renewable generation capacity to meet its 33 percent RPS goal. The first solution assumes that all locations must continue to have at least the capacity that was already installed at the start of the sample period,

⁷https://www.californiasolarstatistics.ca.gov/reports/cost_vs_system_size/

April 1, 2011. The second solution only assumes that capacities at all renewable resource locations must be non-negative.

In both instances we solve the Lagrangian (5), in the first case with $K_j \geq K_j^e$ for all j , and in the second case with $K_j \geq 0$ for all j . We use the realized variable cost of producing electricity each hour of the year to produce the realized residual demand during that hour, $C^h(D_h - R_h)$ in place of $E[C^h(R_h - R_h)]$ and the realized value of $A^h(R_h^w, R_h^s, D_h)$ in place of $E[A^h(R_h^w, R_h^s, D_h)]$ in (5). In the modified RPS constraint (14), we replace $E[D_h]$ and $E[RE_h]$ with the actual values of D_h and RE_h . Finding the solution to (5) requires solving a bound-constrained, nonlinear program with a single linear constraint (the RPS constraint). Comparing our two optimal renewable expansion solutions in Table 5, we find that the total hourly cost of the $K_j \geq 0$ solution is \$1,465,200 per hour, whereas the total cost of the $K_j \geq K_j^e$ solution is \$1,514,200 per hour, a less than 4 percent increase. The cost saving in the $K_j \geq 0$ solution occurs in part because renewable generation in that case relies entirely on wind power. Specifically, the $K_j \geq 0$ solution requires 23,142 MW of wind generation capacity. The $K_j \geq K_j^e$ requires a total of 24,648 MW of wind and solar capacity, of which solar capacity amounts to 499 MW. The difference of 1,506 MW is less than the installed capacity of wind and solar in our base year of 2011 of 3,539 MW. The result implies that more than half of this installed capacity would remain if California was able to start from zero capacity at all wind and solar locations and meet its RPS goals. These findings are a striking difference to actual expansion in solar and wind power in California. More than two-thirds of the capacity increase between 2002 and 2017 was solar power. The findings suggest that there has been overinvestment in solar power, but also at some wind locations because there is less installed wind power in the $K_j \geq 0$ solution than the $K_j \geq K_j^e$ solution. Tables 6 and 7 report similar results for different discount rates. In Section 5, we will show that the 5 locations that have the highest expected revenue per MW installed capacity are wind locations. The main reason why the socially efficient solution does not involve solar power under the $K_j \geq 0$ constraint is because capacity factors are too low compared to the investment cost to justify investment. Those numbers would likely change if the investment costs of solar power were smaller.

We can compute the optimal locational marginal network tariffs for each renewable resource location in California as described in the previous section. We consider the case where tariffs are only designed to internalize the network interconnection costs and the ancillary services costs, and do not account for any inefficient subsidies of renewable energy (alternatively, the support system is efficient). In this case, β_j only depends on the first term of (12), which equals

$$\beta_j = \frac{1}{H} \sum_{h=1}^H E\left[\frac{\partial A^h(R_h^{w*}, R_h^{s*}, D_h)}{\partial R_h^w} f_{jh}\right] \quad (16)$$

if j is a wind location and

$$\beta_j = \frac{1}{H} \sum_{h=1}^H E\left[\frac{\partial A^h(R_h^{w*}, R_h^{s*}, D_h)}{\partial R_h^s} f_{jh}\right] \quad (17)$$

if j is a wind location.

Figure 6 plots a histogram of the locational marginal network tariffs associated with the marginal expected ancillary services cost, i.e. the β_j 's associated with (16) and (17), at each of the 53 solar and wind locations in California for the $K_j \geq K_j^e$ solution, and for three different discount rates. Most of the marginal tariffs are in the range \$0.10 to \$0.25 per hour of the year per MW installed capacity. In net present value, these numbers translate into a total increase in the network tariff in the range of \$7.5 to \$18.6 per KW installed capacity in the baseline specification of $r = 0.10$ and a 20 year life span of the investment, to be compared with the estimated investment costs of the renewable generation units. Under the assumption that the total investment cost of a wind power plant is \$2,000 per KW, and the network interconnection cost amounts to ten percent of the total investment cost, accounting also for the marginal ancillary services costs can add between 4 and 9 percent to the network tariff of a wind power plant. These increases in the network tariff certainly are not negligible, but also not so large that they would substantially reduce the profitability of the investment. We would also expect these magnitudes to change in a more detailed model of the California electricity market and to increase with increasing shares of renewables in the system.

There is also substantial variation in the size of the marginal tariffs. They differ by multiples as high as four to one across renewable resource locations. Marginal tariffs are even negative at some locations. A negative number means that an increase in the volume of installed capacity at that location reduces the total expected ancillary services cost, and that investment at the location therefore should be subject to a discount in the network tariff relative to the cost of interconnecting capacity at that location. By implication, the efficient way to reduce ancillary services costs does not necessarily involve spreading renewable generation over a larger number of locations, but can instead involve increased concentration at particularly suitable locations.

Figure 7 plots the histogram of the same component of locational marginal network tariffs for the $K_j \geq 0$ solution. The two histograms are quite similar, which is not surprising given the similarity of the two optimal solutions. However, the locational marginal network tariffs now are smaller and more often negative. Hence, the concentration effect appears to be more pronounced for the $K_j \geq 0$ solution.

The confidentiality of the renewable energy locations prevents us from reporting characteristics of specific locations, but we are able to present plots as function of features of each location. Figure 8 plots the locational marginal network tariff associated with the marginal expected ancillary services costs against the annual average hourly capacity factor at that location for the $K_j \geq K_j^e$ solutions, and for different discount rates. Figure 9 plots the same marginal tariff against the annual

standard deviation of the hourly factor at that location for this same solution. The two figures reveal systematic differences between solar power and wind power. The marginal tariffs for solar power are positive and linearly increasing both in the mean capacity factor and its standard deviation. Differences in capacity factors and their standard deviation appear to be main explanations for differences in the efficient locational marginal network tariffs across solar locations. The picture is very different for wind power. The marginal network tariffs for wind power are more often negative. Also, there is no clear relationship between the magnitude of the tariff at a location and the mean capacity factor or its standard deviation. Instead, there can be substantial differences between different wind locations that have very similar characteristics in terms of their expected capacity factor or standard deviations of the capacity factor. This heterogeneity is particularly visible for locations that are very windy (so that the mean capacity factor is high) or have large wind variability.

Figure 10 plots the same marginal locational network tariff against the annual load-factor weighted average locational marginal price at the $K_j^* \geq K_j^e$ solution. Wind power locations are low-price locations, and solar power locations are high-price locations, but there is no discernible relationship between electricity prices and network tariffs. These results suggest that locational marginal prices cannot be used to predict efficient locational marginal network tariffs.

Figures 11-13 repeat these same three figures for the $K_j \geq 0$ solution with qualitatively similar results.

5 The Cost of Non-Optimal Policies to California

This section compares the cost of alternative policies for attaining California’s 33 percent RPS goals relative to the optimal policy. To determine the potential cost of not pursuing an optimal interconnection policy, we compute the compliance cost for several plausible alternatives.

We consider two different approaches. The first computes the dollar per MW of annual revenue from producing renewable energy at each location valued at the California ISO’s real-time price for that location for all locations in California. We then restrict all new capacity investments to the five highest dollar per MW of annual revenue locations. We run this scenario for the $K_j \geq 0$ constraints. Specifically, we solve (5) restricting the set of locations where investment can take place to the top five most profitable locations.

Given that locational prices are observable and a number of private companies sell information that allows a prospective investor to estimate fairly accurately the annual output at that the location, the information necessary to executive this RPS compliance path is readily available. We experimented with a larger number than five locations, but found the results were not appreciably different from those obtained with a smaller number of locations.

The second expansion scenario assumes that all locations scale up their existing capacity until the 33 percent RPS constraint is met. This solution simply finds the smallest value of γ , a scalar

greater than one, such that the modified RPS constraint (14) is satisfied when all values of K_j^e are multiplied by the γ . We recognize that is an extremely naive expansion strategy, but include it as an upper bound on how costly non-optimal expansion strategies would be.

Results are reported in Table 5. For the five-most-profitable-locations solution for the $K_j \geq 0$ constraints, the total hourly cost is \$1,484,900, which is only slightly higher than the most efficient solution for this case. In particular, the solution does not involve building any solar power and demonstrates the potential efficiency of concentrating wind power production to a few locations even in the presence of ancillary services costs. These results support the view that as long as new entrants focus on the most profitable locations, they should be able to come close to the optimal configuration. This outcome is not guaranteed because the new entrants will have to find the optimal mix of capacity at each of these locations, which is what the efficient network tariffs should deliver. Nevertheless, by restricting attention to just these locations, solutions very close to the social optimum can be found.

It is interesting to note that in terms of installed capacity, the solutions that invest only at the five most profitable locations are able to satisfy the RPS goals with less investment in renewable generation capacity than the socially efficient solutions. For the $K_j \geq 0$ solution, the five-most-profitable-locations solution requires, 22,266 MW, versus 23,142 MW for the least cost solution.

The solution that scales up the existing renewable capacity at all locations by the same factor, $\gamma > 1$, is significantly more expensive and requires much more renewable capacity. The total cost per hour is \$2,065,700 and the total amount of installed capacity is 40,731 MW. This result demonstrates that expansion policies that do not consider the factors we discuss can lead to substantially more expensive paths to compliance with the RPS.

6 Conclusions

Ancillary services costs have in many regions become increasingly important because of the rapid increase in intermittent renewable energy production brought about by renewable energy mandates. The traditional approach to recovering ancillary services costs as a per unit charge on demand may need to be revisited because where renewable generation units locate influences the magnitude of these costs. We propose locational marginal network tariffs for renewable generation as a way to provide incentives for more efficient renewable generation locational decisions.

Whether it is necessary to impose such tariffs on the renewable generation owners by regulatory mandate, or if network owners would voluntarily introduce such tariffs, is likely to depend on the scope of the tariffs, the operational responsibilities of networks owners and on the regulatory regime. For instance, if the only purpose of the network tariff is to cover the direct network interconnection costs and system balancing costs, then a network owner with system operation responsibility (such as a TSO) operating under a revenue cap would have an incentive to introduce the desired locational marginal network tariff because this would be a cost-minimizing tariff for the network owner itself.

Locational marginal network tariffs could reduce or replace standard renewable support mechanisms that pay per unit of electricity produced, such as feed-in tariffs, tradable green certificates and production tax credits. Instead, renewable resource owners would receive a dollar per MW payment each hour of the year for each MW of capacity interconnected at that location. This solution would eliminate inefficient renewable production decisions caused by the standard support mechanisms. Renewable resource owners would no longer have an incentive to produce at negative wholesale prices, as they do with incentive schemes that remunerate on the basis of MWh produced. Instead, they would receive the \$ per MW payment per hour regardless of how much electricity they actually produce and therefore agree to cease production when prices are negative. Operating the unit would then be the responsibility of the network owner.

Although we are cautious in drawing quantitative conclusions from our stylized empirical analysis, we believe several qualitative conclusions are possible that are likely to hold even with a more realistic model. First, we find significant differences in the values of the efficient locational marginal network tariffs for California’s renewable generation locations and in the tariffs for solar versus wind power. The marginal tariffs differ by multiples as high as four to one across renewable resource locations. Marginal tariffs are negative at some locations, suggesting that renewable generation adds to system stability at those locations and therefore should be subject to discounts in the network tariff relative to the cost of interconnecting the capacity. Second, the absolute levels of the payments to cover marginal expected ancillary services costs are modest. In our baseline specification, the network tariff of a wind power plant can increase by an estimated 4 to 9 percent when adjusted to account for the incremental system costs associated with renewable generation expansion. These combined results support the view that locational marginal network tariffs yield a more cost-effective pathway to meeting renewable goals, by creating incentives for renewable owners to make efficient localization decisions without substantially reducing the overall profitability of investments.

References

- Anderson, John, Gordon Leslie, and Frank A. Wolak**, “Experience and Evolution of Wind Power Project Costs in the United States, <http://www.stanford.edu/~wolak>,” 2017.
- Callaway, Duncan S., Meredith Fowlie, and Gavin McCormick**, “Location, Location, Location: The Variable Value of Renewable Energy and Demand-Side Efficiency Resources,” *Journal of the Association of Environmental and Resource Economists*, January 2018, 5 (1), 39–75.
- Lamp, Stefan and Mario Samano**, “(Mis)allocation of Renewable Energy Sources,” Manuscript, Toulouse School of Economics, January 2019.
- Novacheck, Joshua and Jeremiah X. Johnson**, “Diversifying Wind Power in Real Power Systems,” *Renewable Energy*, 2017, 106 (June), 177–185.

Sexton, Steven, A. Justin Kirkpatrick, Robert Harris, and Nicholas Z. Muller, “Heterogeneous Environmental and Grid Benefits from Rooftop Solar and the Costs of Inefficient Siting Decisions,” NBER Working Paper 25241, 2018.

Shahriaria, Mehdi and Seth Blumsack, “The Capacity Value of Optimal Wind and Solar Portfolios,” *Energy*, 2018, *148* (April), 992–1005.

Tejeda, César, Clemente Gallardo, Marta Domínguez, Miguel Ángel Gaertner, Claudia Gutierrez, and Manuel de Castro, “Using Wind Velocity Estimated from a Reanalysis to Minimize the Variability of Aggregated Wind Farm Production over Europe,” *Wind Energy*, 2018, *21* (3), 174–183.

Wolak, Frank A., “Level versus Variability Trade-offs in Wind and Solar Generation Investments: The Case of California,” *The Energy Journal*, 2016, *37* (SI2), 185–220.

Tables and Figures

Table 1: Annual Moments of Hourly Wind, Solar, and Wind and Solar Output (MWh)

	2013	2014	2015	2016	2017	2018
	Hourly Wind Output (MWh)					
Mean	1033.54	1131.32	999.26	1204.73	1235.28	1597.35
Standard Deviation	843.79	881.27	822.59	918.41	957.56	1161.22
Coefficient of Variation	0.82	0.78	0.82	0.76	0.78	0.73
Standard Skewness	0.39	0.49	0.53	0.41	0.47	0.34
Standard Kurtosis	2.03	2.29	2.18	2.05	2.08	1.92
	Hourly Solar (MWh)					
Mean	315.39	1000.38	1510.80	1910.23	2633.99	2923.06
Standard Deviation	435.64	1290.47	1906.14	2391.94	3257.65	3587.68
Coefficient of Variation	1.38	1.29	1.26	1.25	1.24	1.23
Standard Skewness	1.22	0.84	0.83	0.73	0.69	0.67
Standard Kurtosis	3.50	2.14	2.63	1.86	1.78	1.75
	Hourly Combined Wind and Solar Output (MWh)					
Mean	1348.93	2131.57	2510.06	3114.96	3869.27	4520.41
Standard Deviation	883.40	1461.08	1983.06	2426.76	3258.25	3606.08
Coefficient of Variation	0.65	0.69	0.79	0.78	0.84	0.80
Standard Skewness	0.19	0.45	0.63	0.55	0.60	0.55
Standard Kurtosis	2.32	2.50	2.95	2.07	1.97	1.96

Data Source: California ISO Oasis Web-Site.

Table 2: Wind Output Shortfall Durations (Hours)

	2013	2014	2015	2016	2017	2018
Threshold Value	500 MWh					
Number of durations	162	190	199	212	205	170
Mean	19.19	14.64	16.35	12.82	13.67	13.28
Standard Deviation	38.61	28.55	28.06	22.50	20.79	20.23
Maximum	288	216	209	157	129	119
Threshold Value	1000 MWh					
Number of durations	222	263	227	225	238	199
Mean	20.06	16.22	21.15	18.43	17.50	17.09
Standard Deviation	43.47	39.77	44.65	34.52	29.98	32.46
Maximum	357	430	434	268	243	249
Threshold Value	1500 MWh					
Number of durations	255	267	225	262	244	232
Mean	23.53	21.77	27.63	20.83	22.11	18.91
Standard Deviation	49.25	46.66	73.44	38.39	39.36	35.16
Maximum	374	485	949	290	276	254
Threshold Value	2000 MWh					
Number of durations	185	211	193	218	207	238
Mean	40	33.74	38.66	30.89	31.84	22.78
Standard Deviation	94.26	87.80	92.48	58.66	52.50	45.14
Maximum	856	930	952	399	330	377

Data Source: California ISO Oasis Web-Site.

Table 3: Solar output Shortfall Durations (Hours)

	2013	2014	2015	2016	2017	2018
Threshold Value	500					
Number of durations	348	367	365	367	366	366
Mean	17.61	13.72	13.33	12.93	12.57	12.56
Standard Deviation	13.94	1.92	1.50	1.78	1.78	1.77
Maximum	191	21	17	19	16	17
Threshold Value	1000					
Number of durations	181	365	365	366	367	366
Mean	43.24	14.96	14.01	13.73	13.22	13.10
Standard Deviation	299.07	2.27	1.68	2.28	1.87	1.80
Maximum	4041	43	20	42	18	18
Threshold Value	1500					
Number of durations	30	359	364	365	367	366
Mean	288.23	16.35	14.72	14.27	13.67	13.54
Standard Deviation	1429.85	4.53	2.24	3.35	1.87	1.79
Maximum	7858	66	42	67	19	20
Threshold Value	2000					
Number of durations	1	330	360	363	367	364
Mean	8758	19.35	15.66	14.94	14.04	13.97
Standard Deviation	0	21.57	3.58	4.79	2.10	2.74
Maximum	8758	371	44	94	22	43

Data Source: California ISO Oasis Web-Site.

Table 4: Combined Wind and Solar Output Shortfall Durations (Hours)

	2013	2014	2015	2016	2017	2018
Threshold Value	1000					
Number of durations	231	263	256	228	247	171
Mean	13.54	8.46	9.54	8.73	7.96	9.39
Standard Deviation	27.43	6.08	5.70	5.79	5.49	5.65
Maximum	288	20	18	21	16	17
Threshold Value	2000					
Number of durations	260	388	395	378	368	296
Mean	25.55	11.44	10.94	9.75	9.48	9.02
Standard Deviation	53.44	9.04	5.92	6.50	5.56	6.06
Maximum	637	82	44	66	18	41
Threshold Value	3000					
Number of durations	53	298	356	364	388	380
Mean	160.47	21.42	15.85	14.29	12.51	10.72
Standard Deviation	238.97	42.27	8.57	8.42	5.01	5.94
Maximum	1283	684	140	141	65	44
Threshold Value	4000					
Number of durations	4	191	312	344	360	367
Mean	2188	40.06	20.54	16.94	14.91	14.01
Standard Deviation	1653.46	84.36	30.16	11.69	4.62	5.10
Maximum	4022	922	501	178	66	65

Data Source: California ISO Oasis Web-Site.

Table 5: Total Capacity and Cost in Different Scenarios, $r=0.10$

Scenario Name	Wind (MW)	Solar (MW)	Wind+Solar (MW)	Total Cost
1. $K_{lower} = 0$	23142	0	23142	1465200
2. $K_{lower} = Actual$	24149	499	24648	1514200
3. Top 5	22266	0	22266	1484900
4. Scale up	34986	5745	40731	2065700

Table 6: Total Capacity and Cost in Different Scenarios, $r=0.08$

Scenario Name	Wind (MW)	Solar (MW)	Wind+Solar (MW)	Total Cost
1. $K_{lower} = 0$	23218	0	23218	1382300
2. $K_{lower} = Actual$	24233	499	24732	1424200
3. Top 5	22322	0	22322	1405200
4. Scale up	34986	5745	40731	1899600

Table 7: Total Capacity and Cost in Different Scenarios, $r=0.05$

Scenario Name	Wind (MW)	Solar (MW)	Wind+Solar (MW)	Total Cost
1. $K_{lower} = 0$	23529	0	23529	1266800
2. $K_{lower} = Actual$	24489	499	24988	1298900
3. Top 5	22564	0	22564	1294200
4. Scale up	34986	5745	40731	1669700

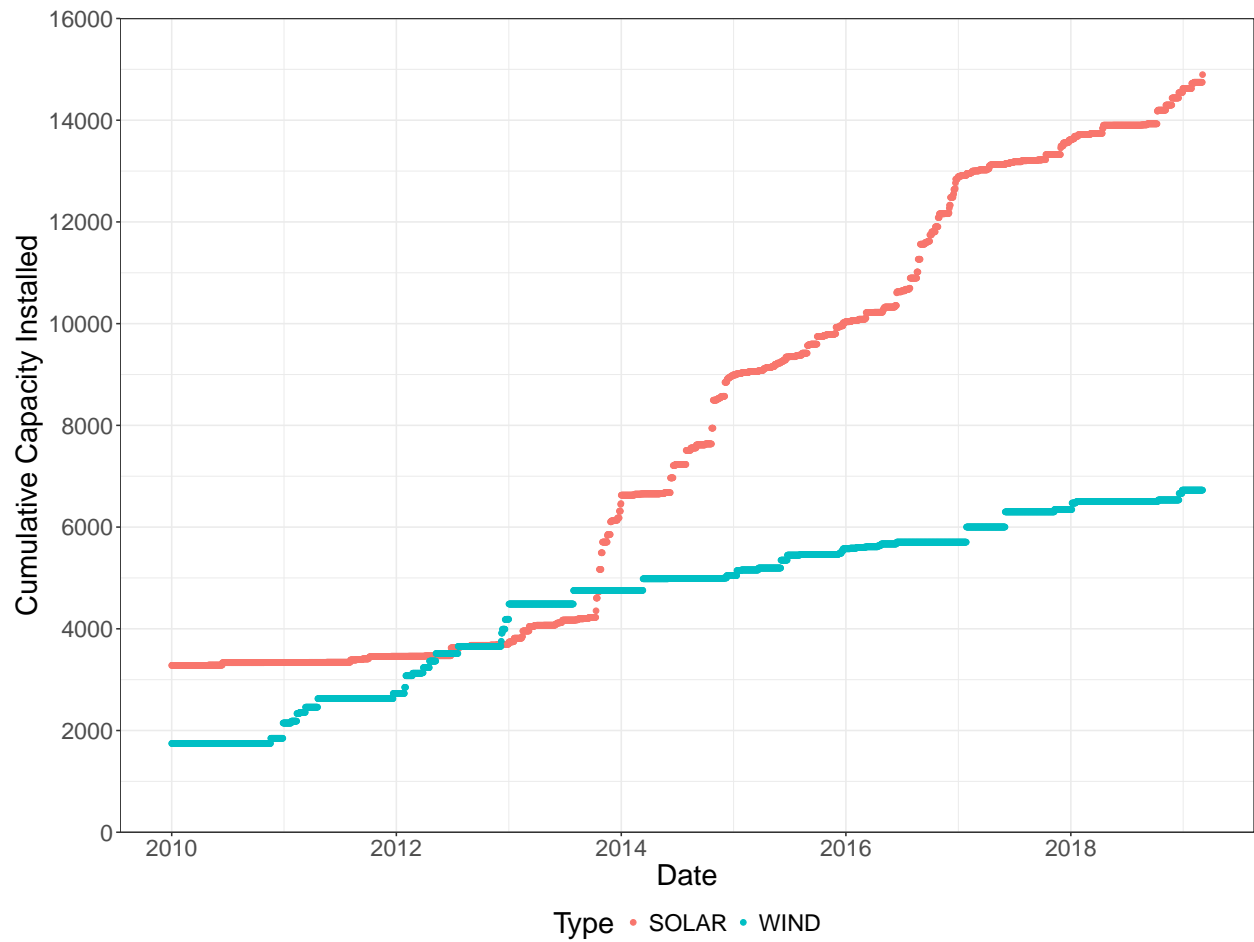


Figure 1: Installed Capacity of Solar and Wind Generation in California ISO Control Area from 2010 through 2018 (MW).

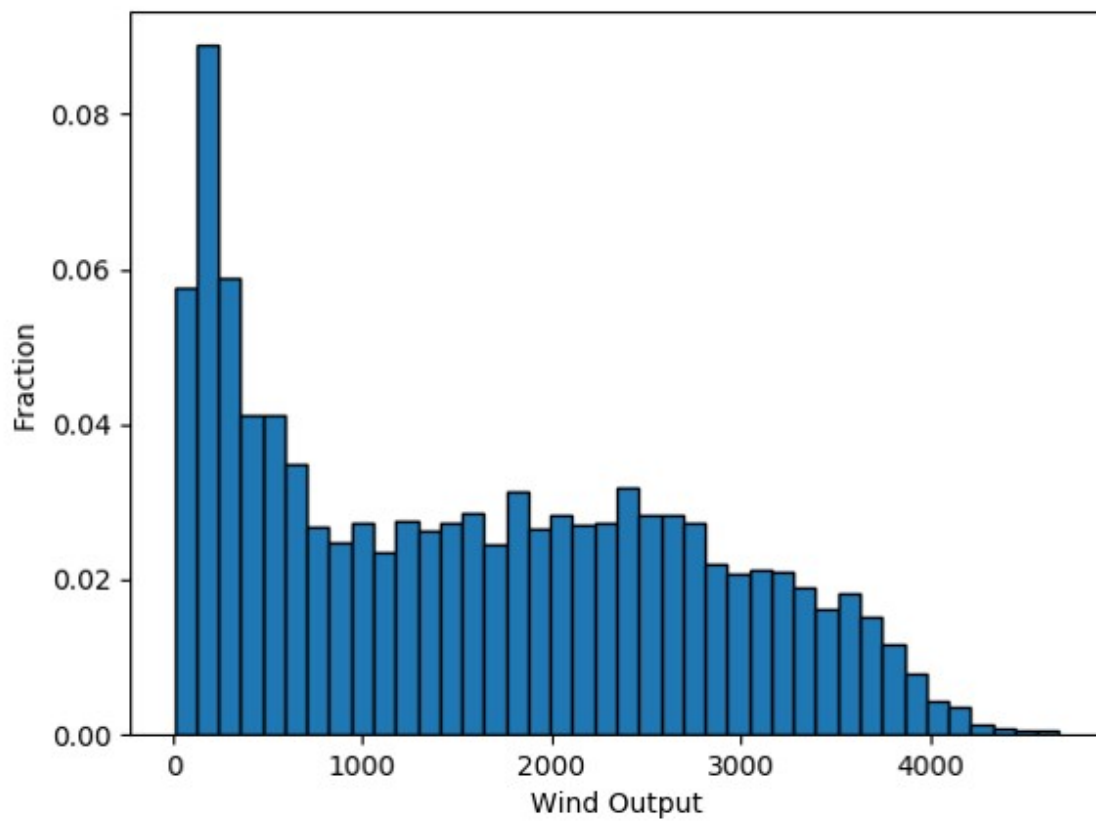


Figure 2: Histogram of Hourly Wind Output in California ISO Control Area in 2018 (MWh).

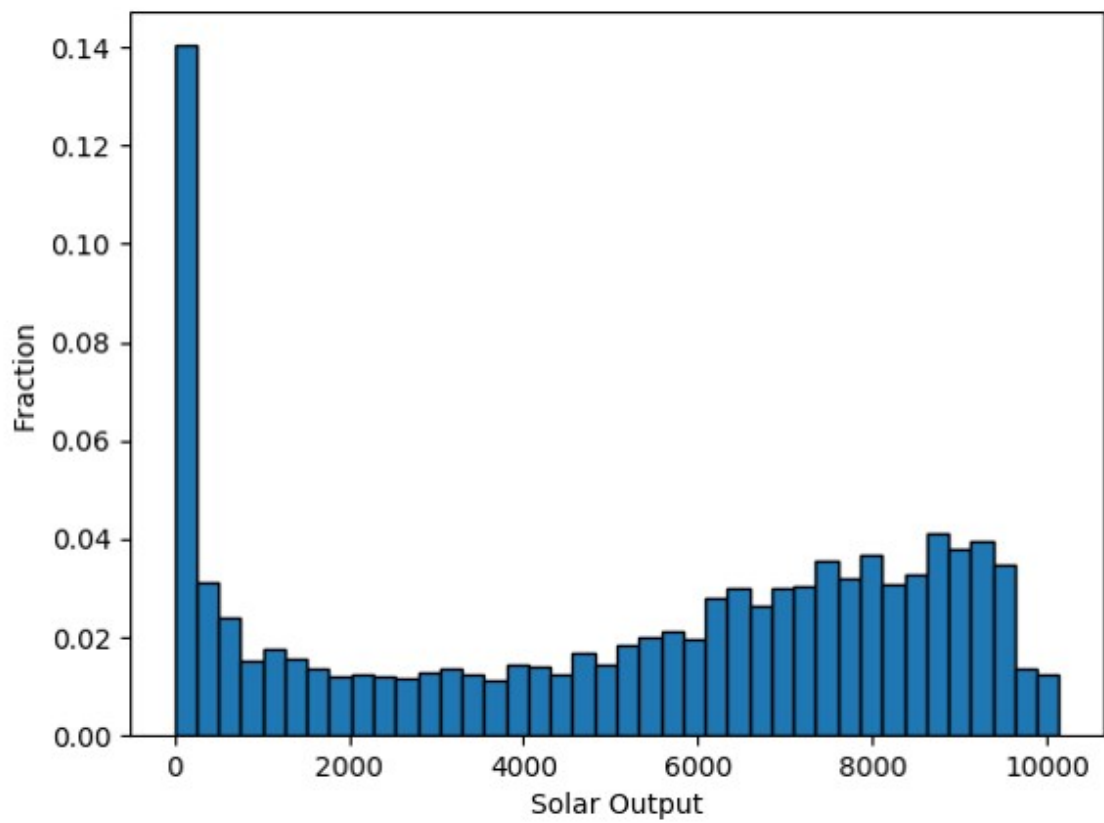


Figure 3: Histogram of Hourly Solar Output in California ISO Control Area in 2018 (MWh).

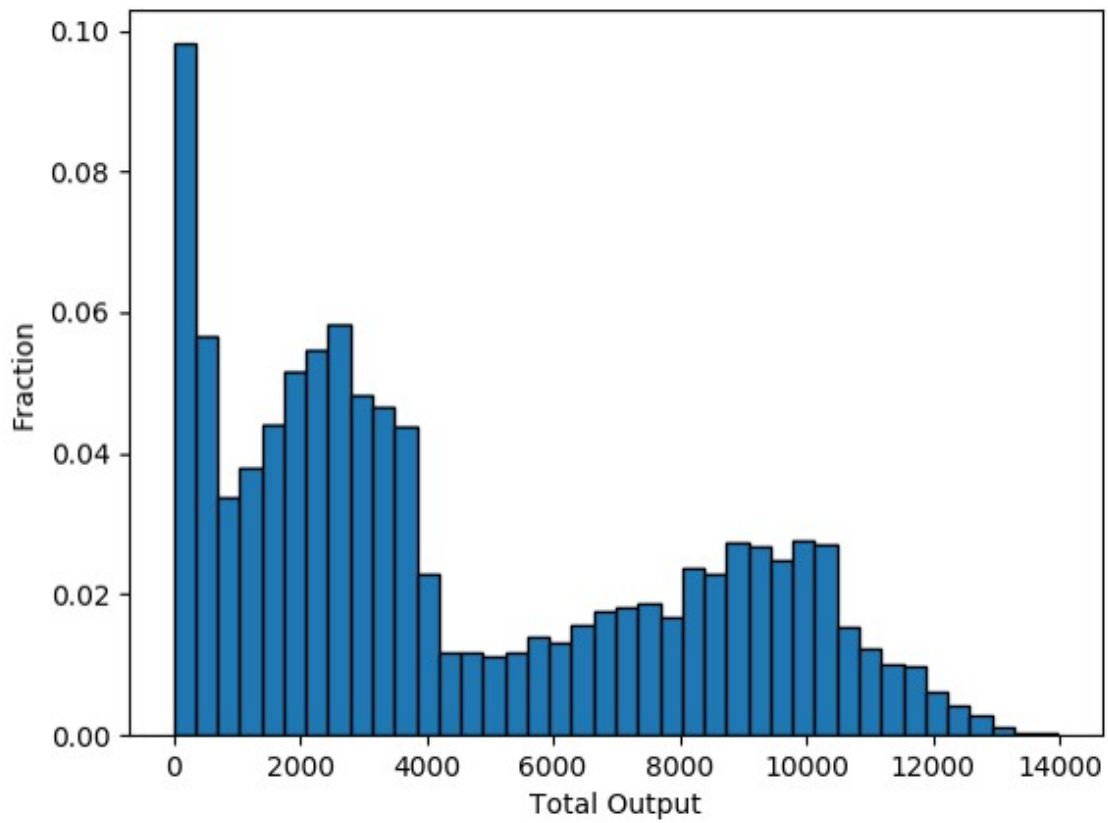


Figure 4: Histogram of Hourly Combined Wind and Solar Output in California ISO Control Area in 2018 (MWh).

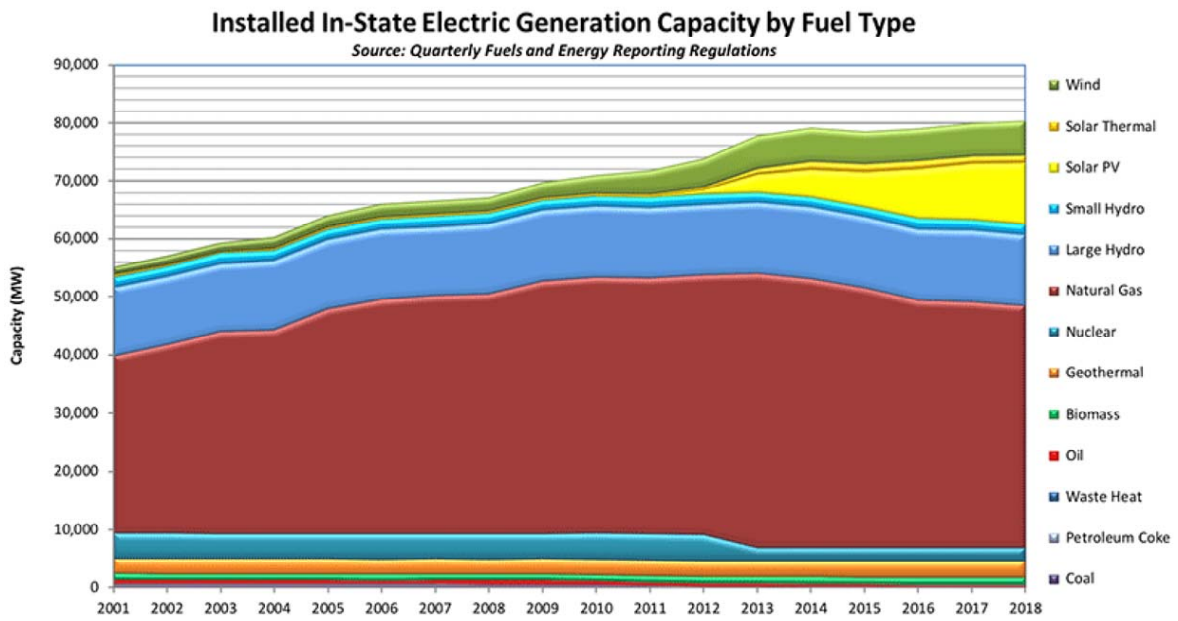


Figure 5: In-State Installed Generation Capacity by Technology (MW), Year End 2001 to 2018.

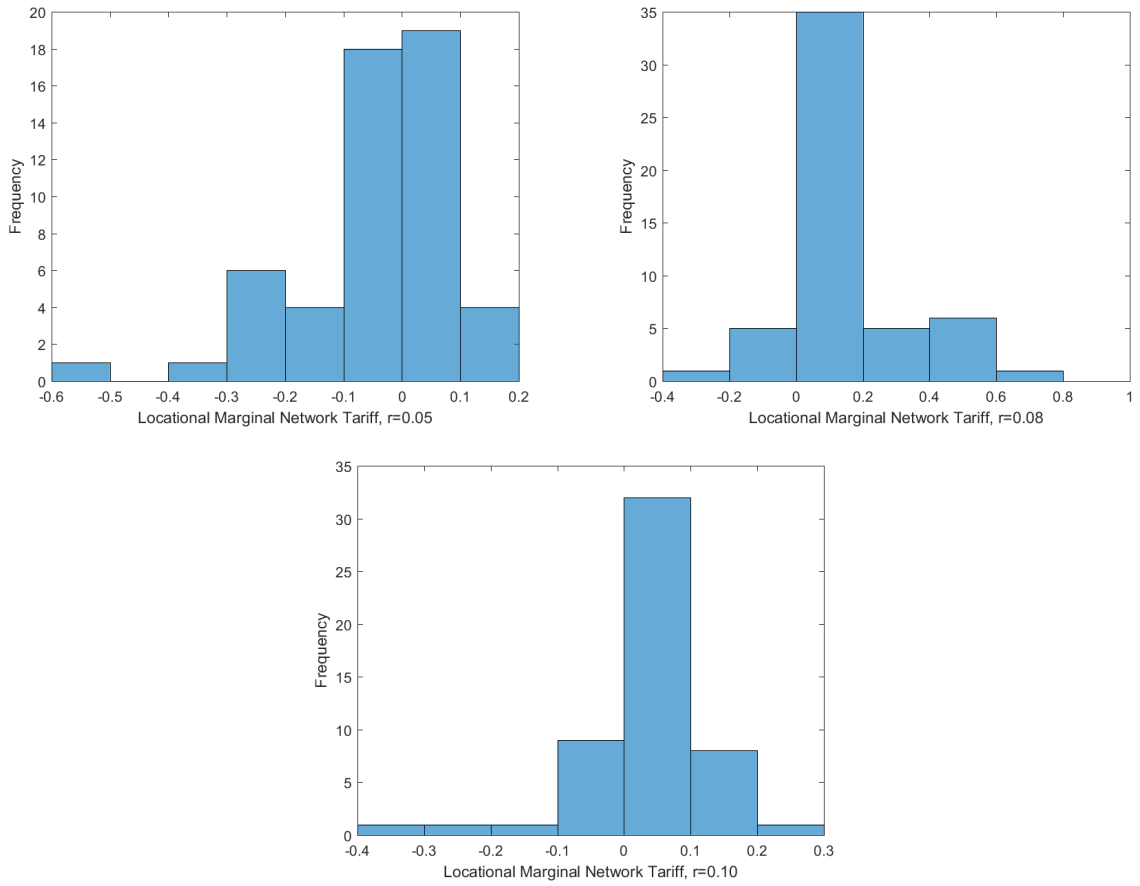


Figure 6: Histogram of Locational Marginal Network Tariffs for the $K_j^* \geq K_j^e$ Solution.

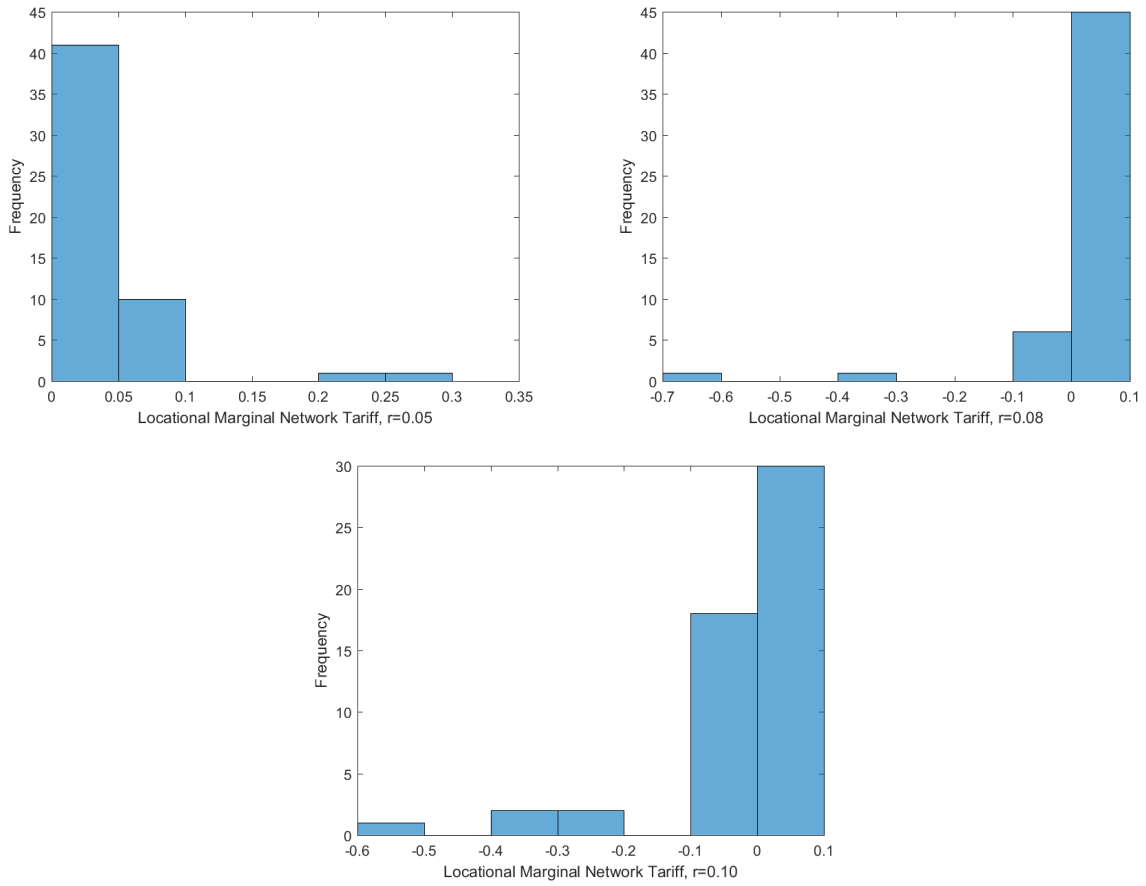


Figure 7: Histogram of Locational Marginal Network Tariffs for the $K_j^* \geq 0$ Solution.

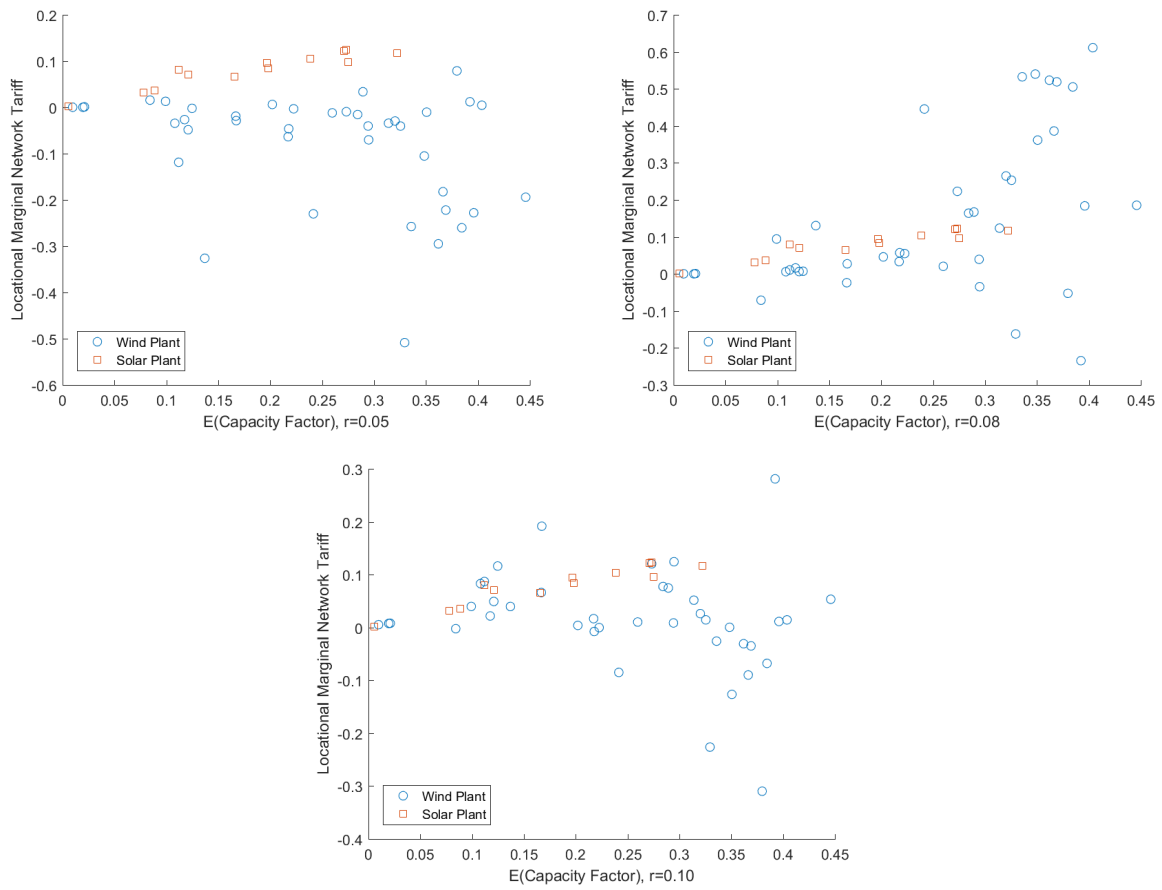


Figure 8: Annual Mean Capacity Factor and Marginal Network Tariff by Location at the $K_j^* \geq K_j^e$ Solution.

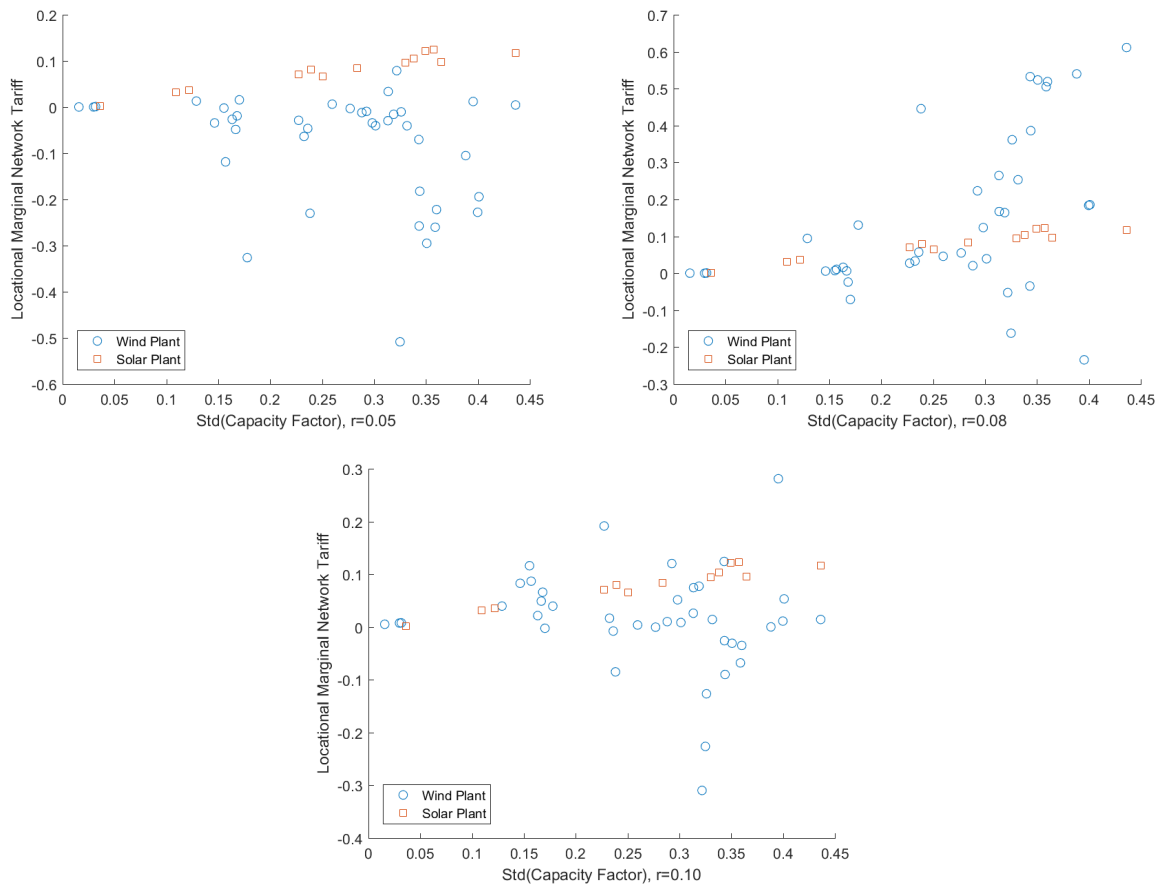


Figure 9: Annual Standard Deviation of Capacity Factor and Marginal Network Tariff by Location at the $K_j^* \geq K_j^e$ Solution.

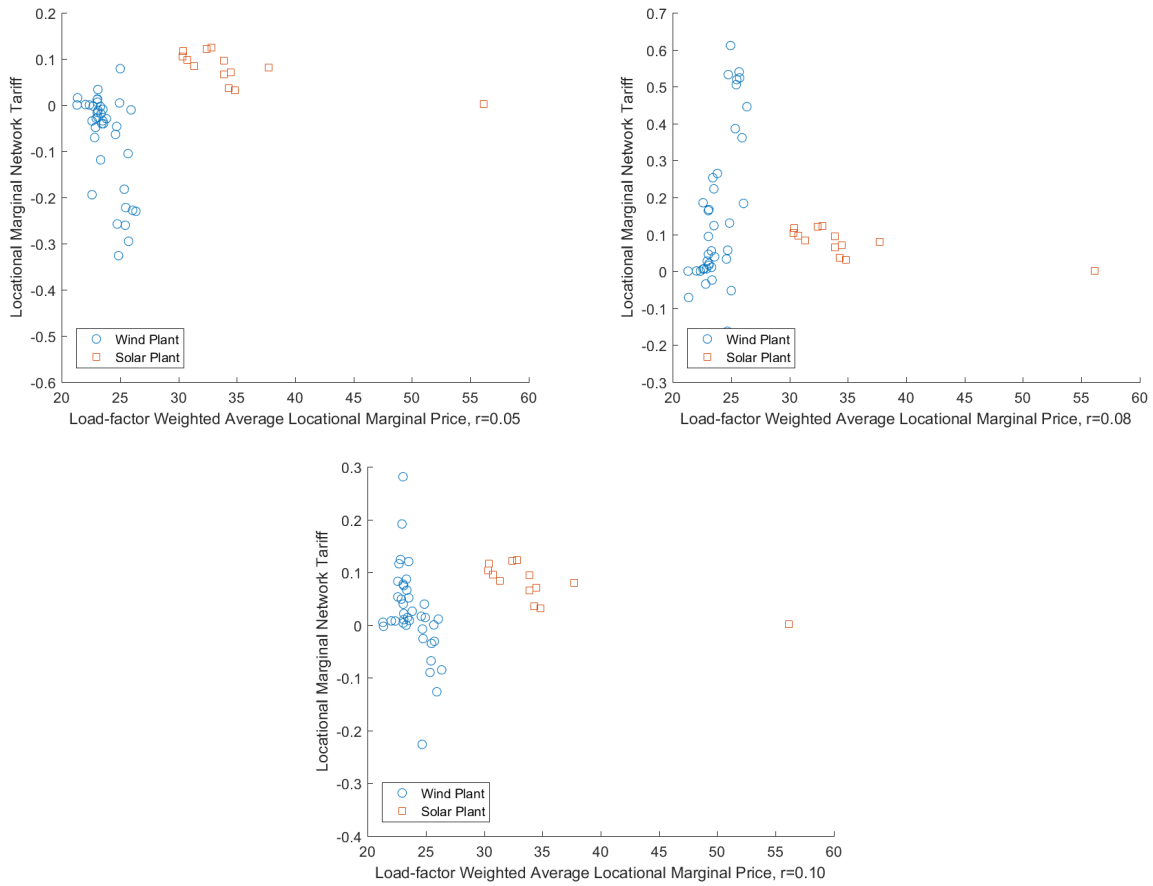


Figure 10: Annual Load-factor Weighted Average Locational Marginal Price and Locational Marginal Network Tariff at the $K_j^* \geq K_j^e$ Solution.

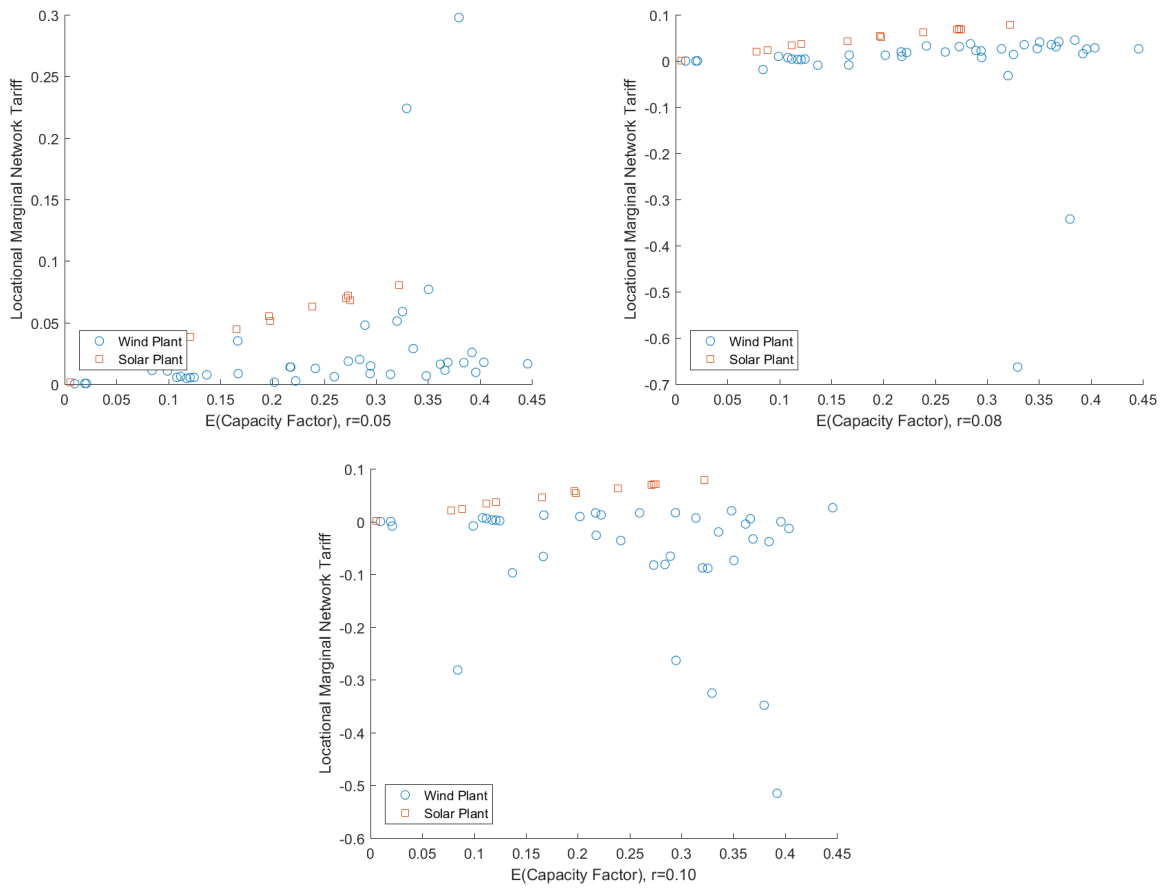


Figure 11: Annual Mean of Hourly Capacity Factor and Marginal Network Tariff by Location at the $K_j^* \geq 0$ Solution.

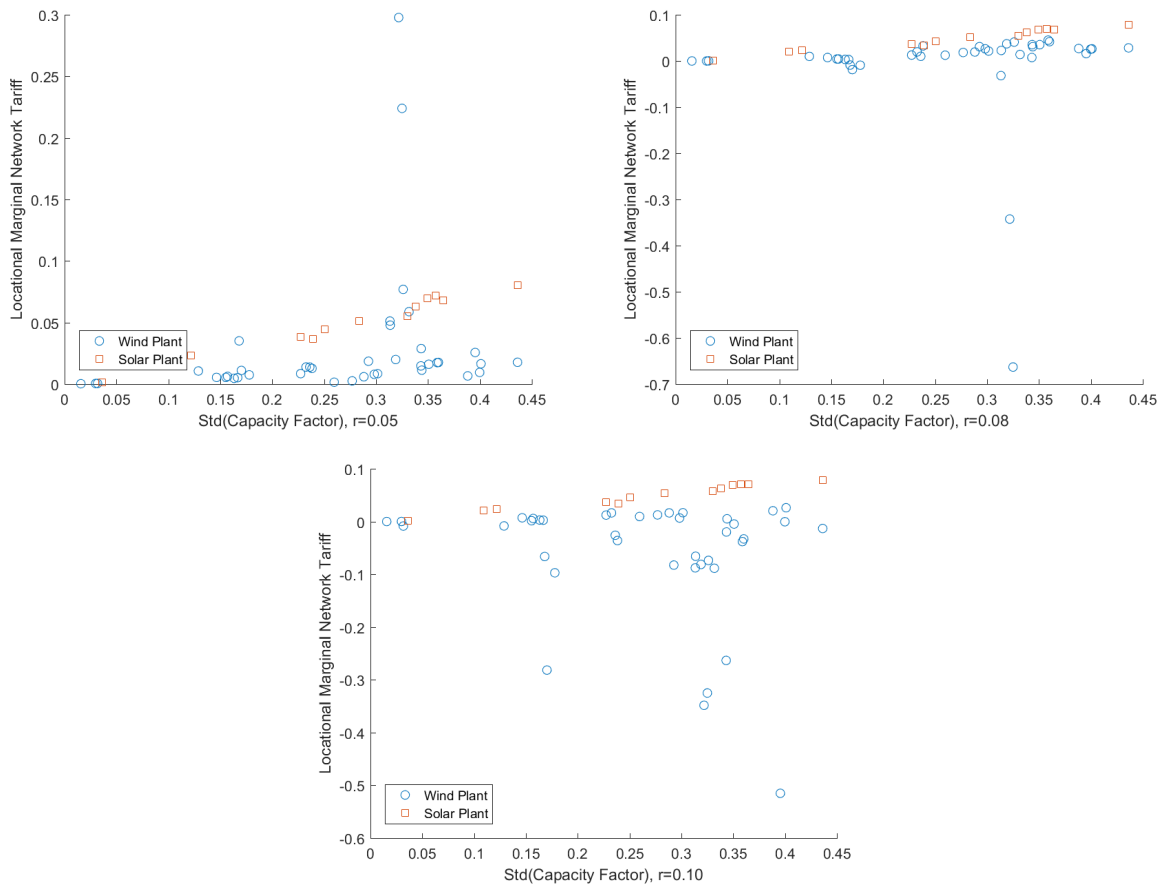


Figure 12: Annual Standard Deviation of Capacity Factor and Marginal Network Tariff by Location at the $K_j^* \geq 0$ Solution.

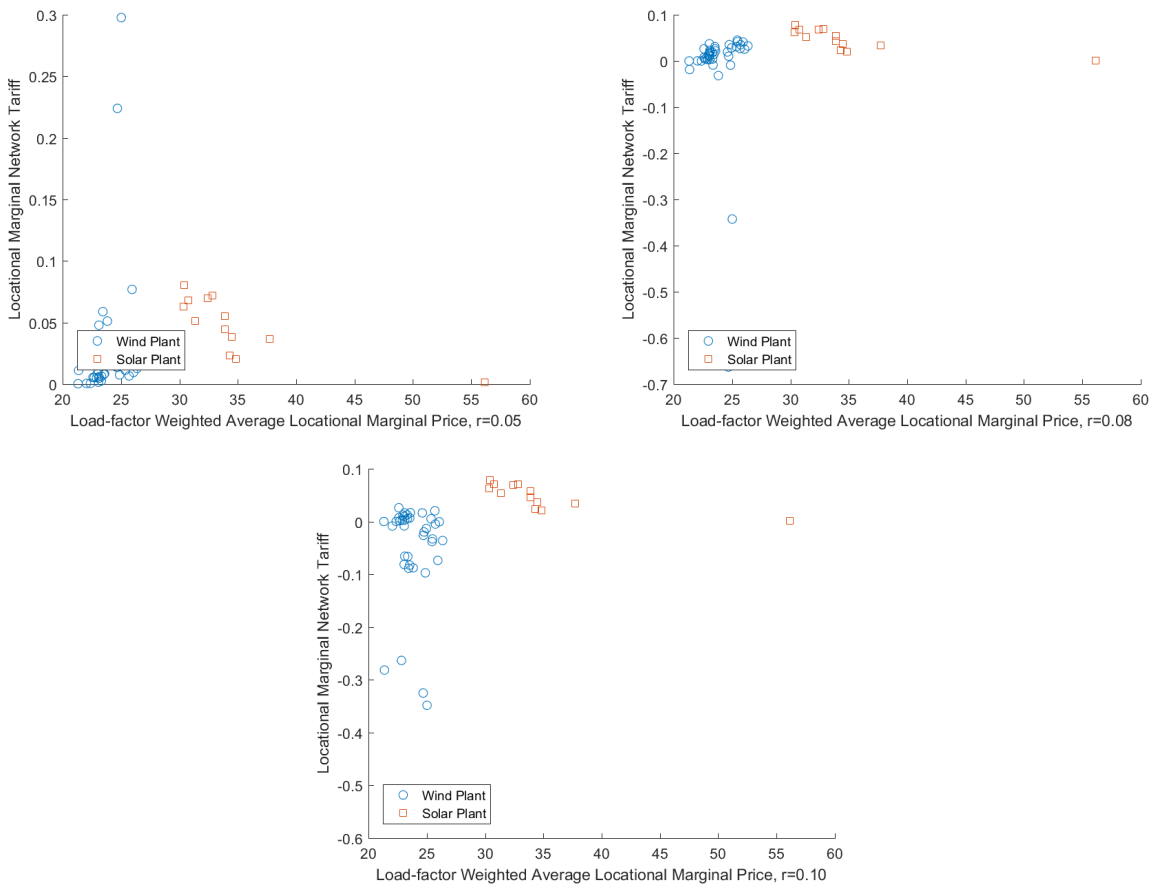


Figure 13: Annual Load-factor Weighted Average Locational Marginal Price and Marginal Network Tariff by Location at the $K_j^* \geq 0$ Solution.

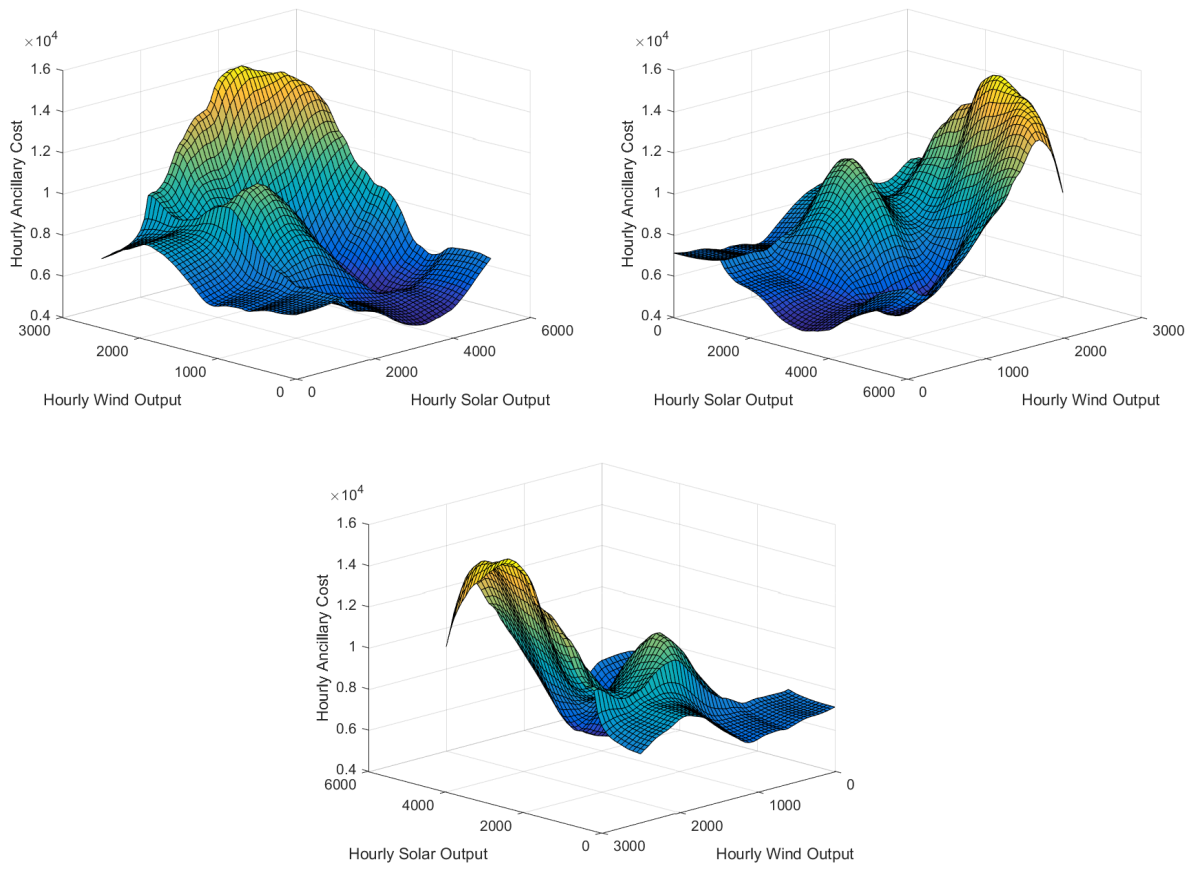


Figure 14: Expected Value of Ancillary Cost $E[A^h(R_h^w, R_h^s, Q_h)]$ as a function of R_h^w and R_h^s for sample mean of Q_h .

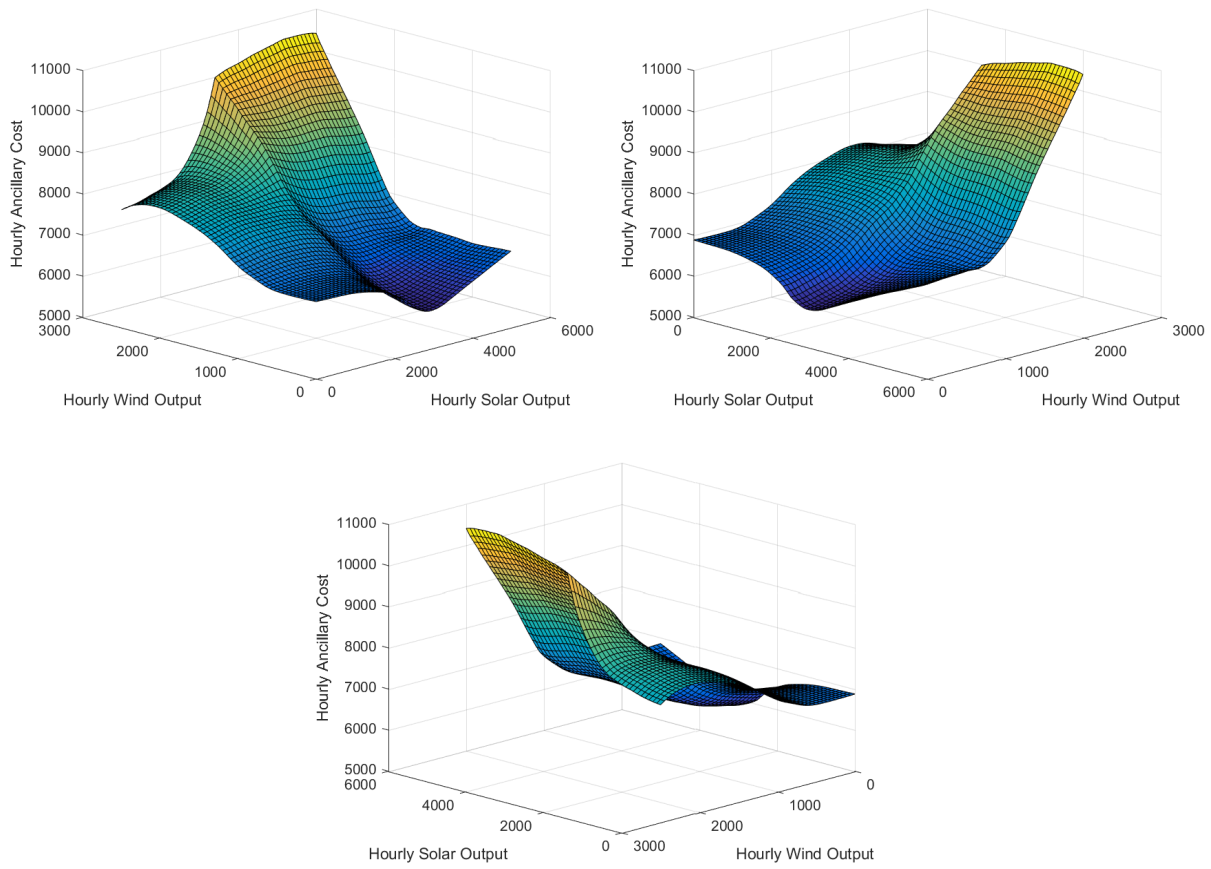


Figure 15: Expected Value of Ancillary Cost $E[A^h(R_h^w, R_h^s, Q_h)]$ as a function of R_h^w and R_h^s for sample mean of Q_h with double the bandwidth compared to Figure 14.